FOSSIL ENERGY

DOE/BC/15190-1
(OSTI ID: 800795)

# 3-D RESERVOIR AND STOCHASTIC FRACTURE NETWORK MODELING FOR ENHANCED OIL RECOVERY, CIRCLE RIDGE PHOSPHORIA/TENSLEEP RESERVOIR, WIND RIVER RESERVATION, ARAPAHO AND SHOSHONE TRIBES, WYOMING

Semi-Annual Report
May 1, 2000-October 31, 2000

By:
Paul R. La Pointe
Jan Hermanson
Thorsten Eiben

Date Published: September 2002

Work Performed Under Contract No. DE-FG26-00BC15190

Golder Associates, Inc.
Redmond, Washington

**National Energy Technology Laboratory**
**National Petroleum Technology Office**
**U.S. DEPARTMENT OF ENERGY**
**Tulsa, Oklahoma**

DOE/BC/15190-1
Distribution Category UC-122

# 3-D Reservoir and Stochastic Fracture Network Modeling for Enhanced Oil Recovery, Circle Ridge Phosphoria/Tensleep Reservoir, Wind River Reservation, Arapaho and Shoshone Tribes, Wyoming

By
Paul R. La Pointe
Jan Hermanson
Thorsten Eiben

September 2002

Work Performed Under DE-FG26-00BC15190

Prepared for
U.S. Department of Energy
Assistant Secretary for Fossil Energy

Virginia Weyland, Project Manager
U.S. Department of Energy
National Energy Technology Laboratory
National Petroleum Technology Office
One West Third Street, Suite 1400
Tulsa, OK 74103

Prepared by
Golder Associates Inc.
18300 NE Union Hill Road, Suite 200
Redmond, WA 98052

GeoData Services
P.O. Box 1123
Coos Bay, OR 97420

**Table of Contents**

**List of Graphical Materials**

**List of Tables**

## ABSTRACT

This report describes the progress and results made in fulfillment of contract DE-FG26-00BC15190, "3-D Reservoir and Stochastic Fracture Network Modeling for Enhanced Oil Recovery, Circle Ridge Phosphoria/Tensleep Reservoir, Wind River Reservation, Arapaho and Shoshone Tribes, Wyoming" during the first 6 months of the project. The goal of this project is to improve the recovery of oil from the Circle Ridge Oilfield, located on the Wind River Reservation in Wyoming, through an innovative integration of matrix characterization, structural reconstruction, and the characterization of the fracturing in the reservoir through the use of discrete fracture network models. Progress and results have been obtained during this period for several tasks: Task 1 – Petrophysical Analysis; Task 2.1 – Compilation of existing data; Task 2.2 – Core/FMI Data Analysis; Task 2.3 – Field Data Collection & Analysis; Task 2.4 – Construction of Balanced Cross-sections; Task 5.1 – Project Web Site; Task 5.3 – Workshops for Tribes. Task 2.4 was not scheduled for initiation in the first six months, but due to ongoing restructuring at team member Marathon Oil, this work was accelerated to take advantage of Marathon staff who might not be continuing with the Marathon. In order to accommodate this additional work, some of the analysis work for the field data and subsurface data that does not require Marathon expertise was deferred until the remainder of 2000. It is not anticipated that this slight change in the schedule will have any negative impact on the technical scope of the work, its cost or meeting the schedule of other deliverables in the project.

Task 1 has been completed. Completion has provided the project with a database of tops, matrix porosity and fluid saturations for 134 wells, including 105 wells with data from the overthrust block, and 39 wells with data from the subthrust block. Marathon Oil also provided existing geological and production data for key wells, and acquired new FMI image log data and high resolution production data from an existing well for the project. Fieldwork completed in June and July in the Circle Ridge Field provided two types of data for the project: (1) surface data along three transects to help construct cross-sections across key portions of the field; (2) data on individual fractures taken along scanlines in key formations and structural positions to help relate large-scale structural deformation and lithology to fracture development. The cross-sections are not yet complete, but are in the process of being modeled using three-dimensional palinspastic reconstruction. In June, the project was presented to both Marathon Oil Company personnel in Cody, WY and to tribal members and officials at Fort Washakie, WY. The project website was created and made available for public access in late summer. All available data, presentations and background material to date have been posted to this website.

Key findings to date are: (1) the strategies for deriving matrix properties from older vintage logs has proven successful, greatly expanding the coverage for the reservoir; (2) existing structural models of the Field are generally correct, but insufficient for 3D palinspastic reconstruction. The fieldwork carried out is providing the necessary data for completing the 3D reconstructions; (3) the Gypsum Springs Formation probably forms a major detachment horizon, so that fracture data taken in overlying units may not reflect the fracture pattern in the reservoir units; and (4) preliminary interference test results suggest a strong west-northwest effective permeability anisotropy that does not coincide with the axis of the Field.

A review of the schedule indicates that the project is essentially on schedule despite major restructuring at Marathon Oil Company, and with the timely submission of this report, will have met all scheduled deliverables to this point.

# 1 INTRODUCTION

The first six months of the 3D reservoir and stochastic fracture network modeling for enhanced oil recovery, for the Circle Ridge Field has primarily focused on data collection and preliminary analysis. During this period, there were three active main tasks composed of several active subtasks. The main tasks were Task 1 – Petrophysical Analysis (all subtasks active), Task 2 – Development of the structural conceptual model (subtasks 2.1, 2.2 and 2.3 active), and Task 5 – Technology Transfer (all subtasks active). Due to personnel scheduling considerations relative to Marathon Oil Company's ongoing restructuring, substantial work has also been completed on Task 2.4 – Construction of balanced cross-sections.

At this stage in the project, Marathon Oil Company has provided in-kind contribution of a new FMI image log (and the associated processing) and a spinner and temperature log in one well.

Throughout this report, reference is made to the "overthrust block" and "subthrust block". At this point in the project, a model for the fault block architecture is still under development, and all data points to a configuration more complex than a simple hanging wall/footwall division. In general, this nomenclature is used to distinguish between rock in the hanging wall of the main Red Gully Fault (overthrust) and rock in the footwall (subthrust).

This report does not focus on the regional geological setting, tectonic history or reservoir stratigraphy. While the information on these are important to the project, they are primarily important for the final balanced cross-section reconstruction and especially the interpretation of the fracture data for the construction of the discrete fracture network model of the reservoir. Since these tasks are the focus of the next six month period, detailed discussions of the regional geology, tectonic history and reservoir stratigraphy are deferred to future technical and/or topical reports.

This report follows the outline mandated in Section 4.14 (Guidelines for Organization of Technical Reports (May 1999)) as specified in the contract. The discussion of the experimental work is organized by Task, as are the Results and Discussion section (Section 3).

# 2 EXPERIMENTAL WORK

## 2.1 Overview

The experimental work during the first six-month period of this project falls into five broad areas: petrophysical interpretation; existing and new data collection; field structural geology; 3-D palinspastic reconstruction; and reporting. The experimental work supporting these tasks is described in greater detail in the remainder of this section.

## 2.2 Task 1 – Petrophysical Analysis

### 2.2.1 OVERVIEW

The purpose of the petrophysical work at Circle Ridge was to determine as accurately as possible the original oil in place in the Phosphoria and Tensleep Formations, the primary reservoir units. The results of this analysis will be passed on to the visualization model, which will consist of a 3D image of the reservoir that includes matrix properties and structural elements. The matrix data will be used to determine the original volume of oil in place. The data covers the overthrust area and the five or six downthrown blocks that make up the subthrust part of the field in the northwest area of the field. Not all wells could be analyzed using the same approach due to differences in available log types and quality. As a result, several different analysis approaches were used.

The primary and most accurate analysis approach utilized the MULTIMIN program, which is an optional module to the Paradigm Geophysical Corporation's (http://www.paradigmgeo.com) GeoLog6® log interpretation program. The MULTIMIN program provides for a simultaneous solution for minerals, porosity, and fluids. The analysis requires density, neutron, shallow and deep resistivity logs as a minimum suite for analysis. The algorithms embodied in the software represent the current state-of-the method available for determining porosity and fluid saturation from logs. Fifty wells had the required measurements to run this type of analysis. Thirty-nine of these were in the overthrust and eleven were in the subthrust blocks. Six of the wells contained section from both the overthrust and subthrust, so the total number of wells analyzed was forty-four.

The second most accurate method to assess porosity was to plot density and compensated neutron logs when both were available. This procedure was used when resistivity measurements were lacking, and the MULTIMIN analysis could not be carried out as a result. An accurate porosity can be obtained; however the Phosphoria did require a minor adjustment as will be shown in the body of this report. A total of twelve wells fell into this category, four in the overthrust and eight in the subthrust. Two of the wells contained section from both the overthrust and subthrust so the total number of wells analyzed was ten.

The third most accurate porosity was determined when the only porosity measurement available was the density. It is extremely difficult to determine an accurate porosity with only one measurement. To make some use of this data, a method was developed that derived the best guess porosity and is shown in Section 2.2.4 of this report. Thirty-three wells contained only a density log; twenty-three in the overthrust and ten in the subthrust. Two of the wells contained section from both the overthrust and subthrust, so the total number of wells analyzed was thirty-one.

The last measurement to be addressed is the gamma ray neutron (GRN). The method of getting porosity was determined from the only two wells that contained both the GRN and some other measurement. In these two wells the other measurement was the density. The method is discussed in the body of this report. It was important to utilize the GRN wells due to the shear number that only had this measurement. A total of forty-eight wells are involved, thirty-nine in the overthrust and nine in the subthrust. By including these wells, we gained a lot of information in areas that would not have any porosity coverage at all. It is understood that the accuracy of the GRN porosity is certainly suspect when used alone with no calibrated reference to compare to.

The problems with this measurement will be covered in the body of this report.

The next sections describe in greater detail the results of each of these four types of analyses.

### 2.2.2 MULTIMIN ANALYSIS

Figure 2-1 shows the results of the Phosphoria model that was generated over the first ten to twenty wells that were worked on. These wells were used as a calibration set to allow processing of the remaining wells. MULTIMIN operates on a "model" concept where all parameters for a given formation are saved in a model file. There is a Phosphoria model file and a Tensleep model file.

Another feature of MULTIMIN concerns the oil API and gas specific gravity parameters. These and all other fluid and tool parameters are corrected to reservoir conditions (for example, temperature, pressure, or hole size). Currently MULTIMIN will only handle oil or gas, not a combination of both.

#### *2.2.2.1 Phosphoria Analysis*

The Phosphoria model has the following characteristics:

- The gamma ray was not utilized in determining minerals. The effect of the Uranium mineral on the gamma ray response in the Phosphoria is well known.
- Only calcite and dolomite were chosen for mineral determination. The Phosphoria is usually found to be a clean carbonate.

- The water resistivity for the Phosphoria was adjusted during model determination. By utilizing the Pickett plot (Asquith and Gibson, 1982) during generation of the model, it soon became apparent that these values (shown below) applied across the Circle Ridge field. So, from the Pickett plot:

  Rw: 1 ohmm at 80 degrees F (water resistivity)
  a: 1
  m: 1.8 (cementation exponent for porosity)
  n: 2 (water saturation exponent)

Figure 2-2 shows the Pickett plot for the Phosphoria in well 66-49.
Figure 2-3 presents (in black) the original logs used by MULTIMIN to create the mineral percentages, porosity, and fluid saturations. Also presented (in red) are the reconstructed logs generated by MULTIMIN, which shows how well the model predicts the original data.

As previously mentioned, the gamma ray log was not used in the Phosphoria model to determine the results. Thus there is no predicted gamma ray log in Track 1. However the gamma ray log was used in the Tensleep model, and
Figure 2-3 shows the match over this Formation.
Figure 2-3 covers the same interval as shown in Figure 2-1.

#### *2.2.2.2 Tensleep Analysis*

Figure 2-4 shows the results of the Tensleep model that was generated. The Tensleep model has the following characteristics:

- The gamma ray log was utilized for determining minerals.

- Quartz, dolomite, and illite clay were chosen for mineral determination. The Tensleep also contains traces of heavy mineral, such as pyrite. Since there were an insufficient number of measurements to solve for pyrite, the end point for zero porosity was adjusted upwards from 2.65 to 2.67 in the model for the density to compensate.

- The water resistivity for the Tensleep, like the Phosphoria, was adjusted during model determination in a similar manner (Pickett plot). Figure 2-5 shows the Pickett Plot for the Tensleep Formation.

The following values that worked well for the Phosphoria Formation also worked well for the Tensleep:

Track 1 - MULTIMIN minerals and total volume display
Track 2 - depth in feet
Track 3 - total porosity and fluid content. Area shaded green is percentage of porosity that is unmoved oil, area shaded yellow is percentage of moved oil in the invaded zone. The clear area is percent water saturation in the undisturbed formation.
Track 4 - water saturation
Track 5 - measured hole diameter and density correction

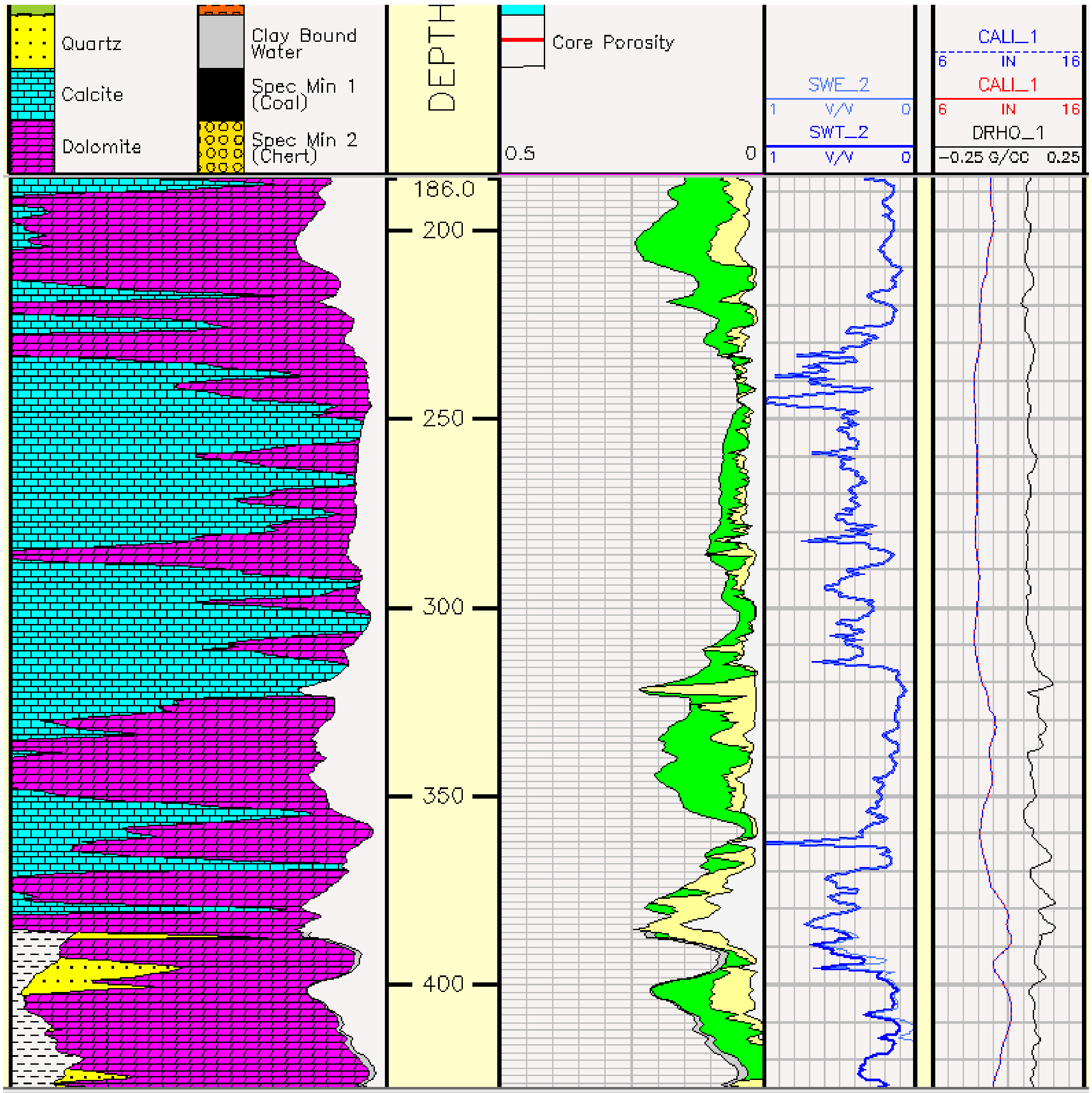


Figure 2-1. Phosphoria MULTIMIN display

Track 1 - black: logged GR    red: MULTIMIN predicted gr
Track 2 - black: logged nphi   red: MULTIMIN predicted nphi
Track 3 - black: logged rhob   red: MULTIMIN predicted rhob
Track 4 - intervals shown
Track 5 - black: logged dt    red: MULTIMIN predicted dt -- no logs shown
Track 6 - black: logged x conductivity    red: MULTIMIN predicted x conductivity
Track 7 - black: logged t conductivity    red: MULTIMIN predicted t conductivity

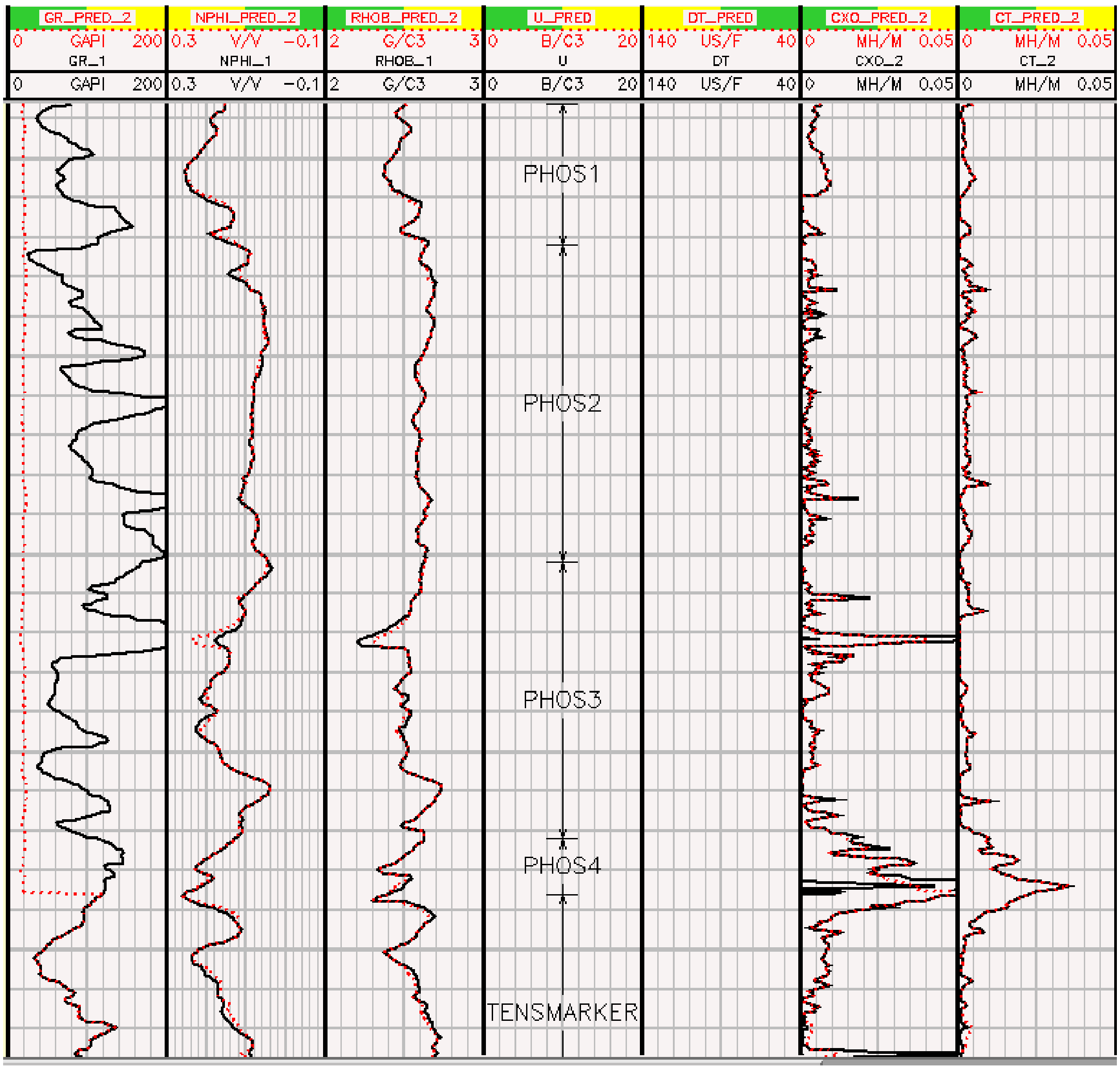


Figure 2-2. Picket Plot for well 66-49, Phosphoria Formation

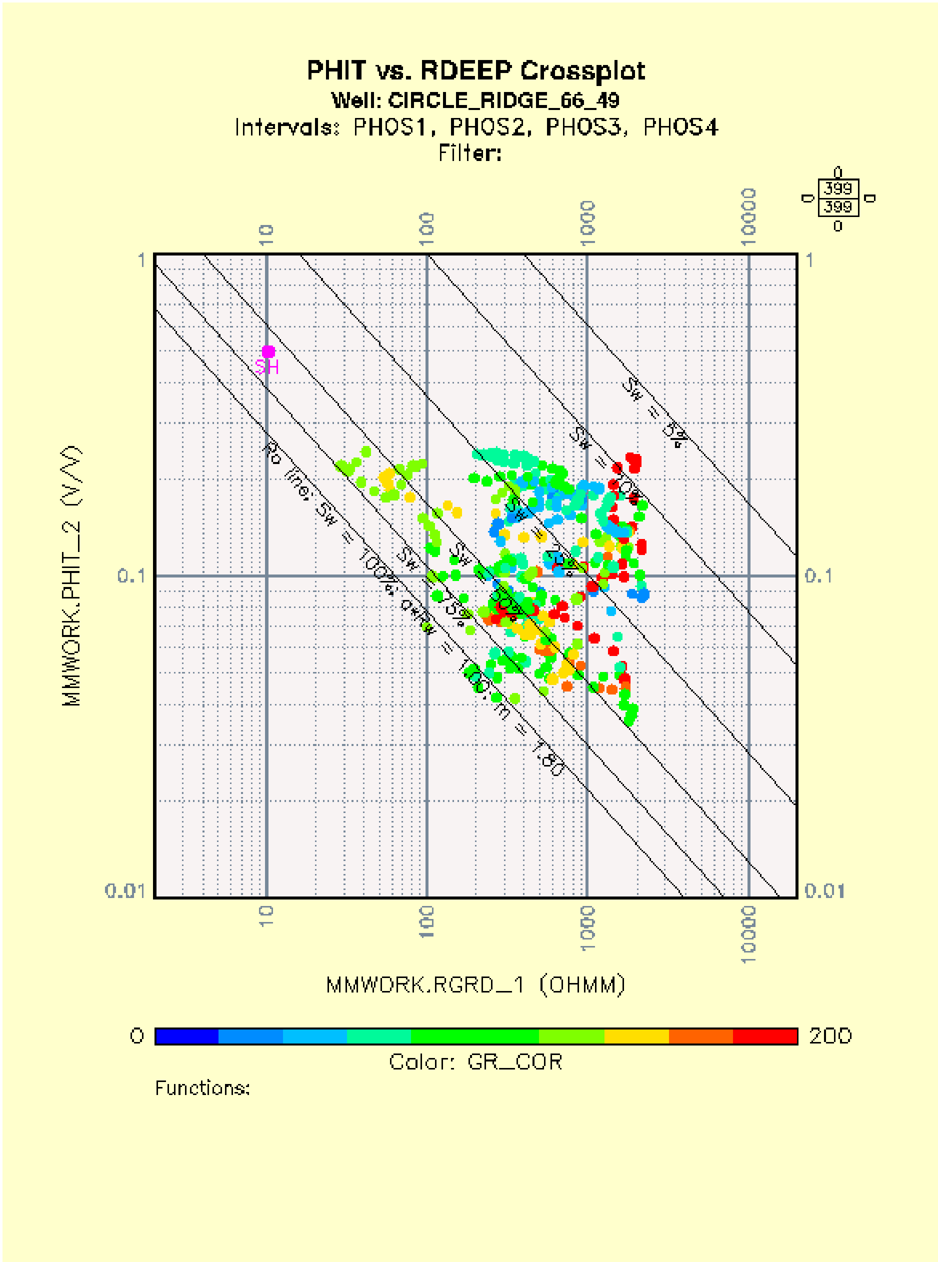


Figure 2-3. Phosphoria MULTIMIN predicted and real logs

| | | |
|---|---|---|
| Rw: | 1 ohmm at 80 degrees F | (water resistivity) |
| a: | 1 | |
| m: | 1.8 | (cementation exponent for porosity) |
| n: | 2 | (water saturation exponent) |

Figure 2-6 presents the reconstructed logs generated by MULTIMIN. The Figure shows that there is a good fit between the predicted logs and the originals. Figure 2-6 covers the same interval as Figure 2-4.

### 2.2.3 POROSITY CROSSPLOTS

This section addresses the methodology used in wells in which the density and compensated neutron logs are the only porosity logs available.

Figure 2-7 demonstrates the "cp1b" function that allows determination of porosity and apparent matrix density from the density and compensated neutron logs in the Phosphoria Formation. Figure 2-8 shows an analogous plot for the Tensleep Formation.

Figure 2-9 shows a comparison of the crossplot porosity in forty-six wells that contain the MULTIMIN porosity for the Phosphoria. A quadratic regression (the blue curve) was performed that corrected crossplot porosity to more closely match the PHIT MULTIMIN porosity. This was used on the ten wells that fit the crossplot criteria.

Figure 2-10 is the corresponding plot to Figure 2-9 for the Tensleep Formation. This plot shows that little correction to the crossplot porosity is required to closely match the MULTIMIN porosity in the Tensleep.

This process was performed on four wells in the overthrust and eight in the subthrust portions of the Circle Ridge Field.

Track 1 - MULTIMIN minerals and total volume display
Track 2 - depth in feet
Track 3 - total porosity and fluid content. Area shaded green is percentage of porosity that is unmoved oil, area shaded yellow is percentage of moved oil in the invaded zone. The clear area is percent water saturation in the undisturbed formation. The red asterisks are core porosity.
Track 4 - water saturation

Track 5 - measured hole diameter and density correction

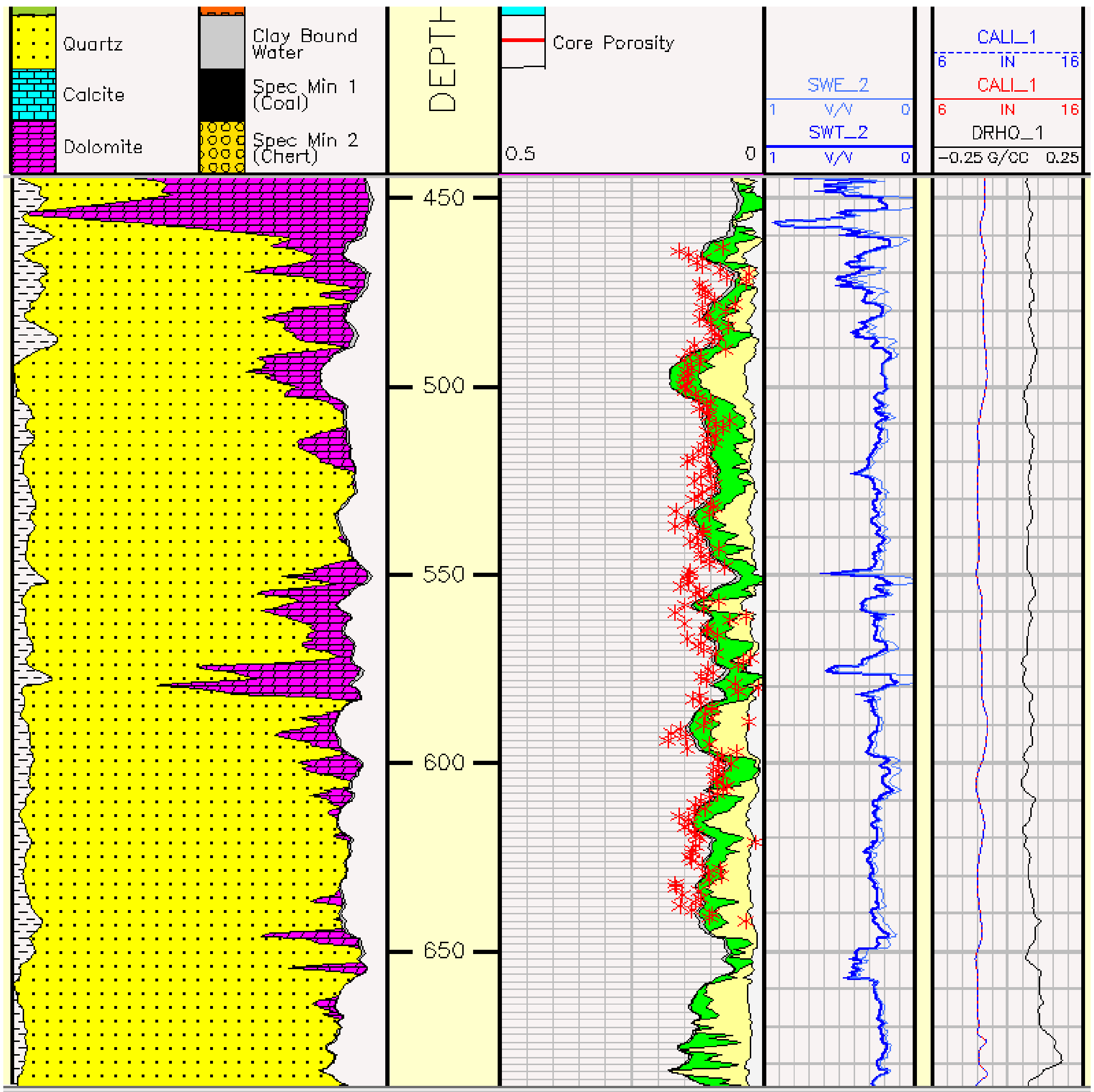


Figure 2-4. Tensleep MULTIMIN display

Track 1 - black: logged GR red: MULTIMIN predicted gr
Track 2 - black: logged nphi red: MULTIMIN predicted nphi
Track 3 - black: logged rhob red: MULTIMIN predicted rhob
Track 4 - intervals shown
Track 5 - black: logged dt red: MULTIMIN predicted dt -- no logs shown
Track 6 - black: logged x conductivity red: MULTIMIN predicted x conductivity
Track 7 - black: logged t conductivity red: MULTIMIN predicted t conductivity

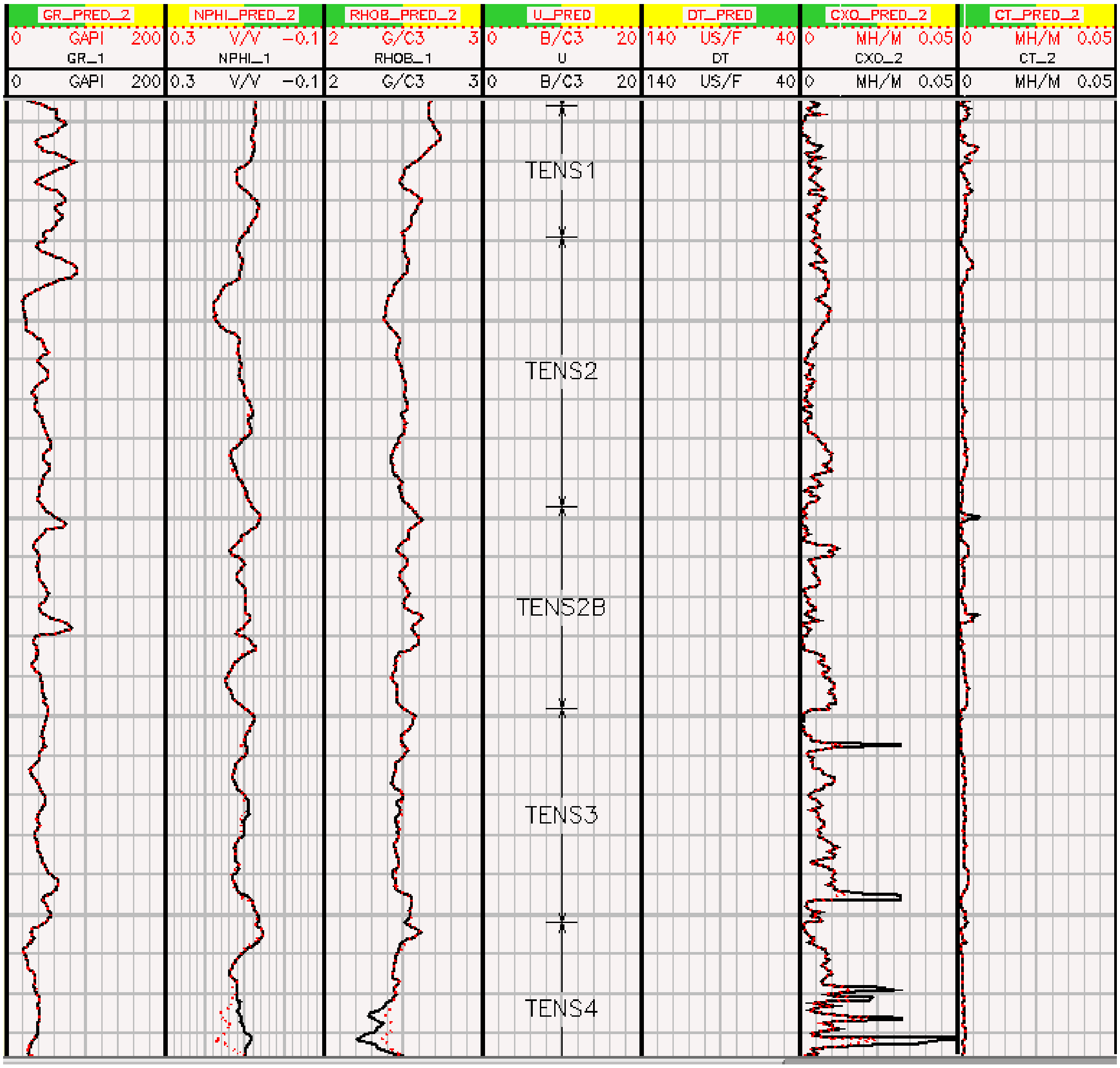


Figure 2-5. Pickett Plot for well 66-49, Tensleep Formation

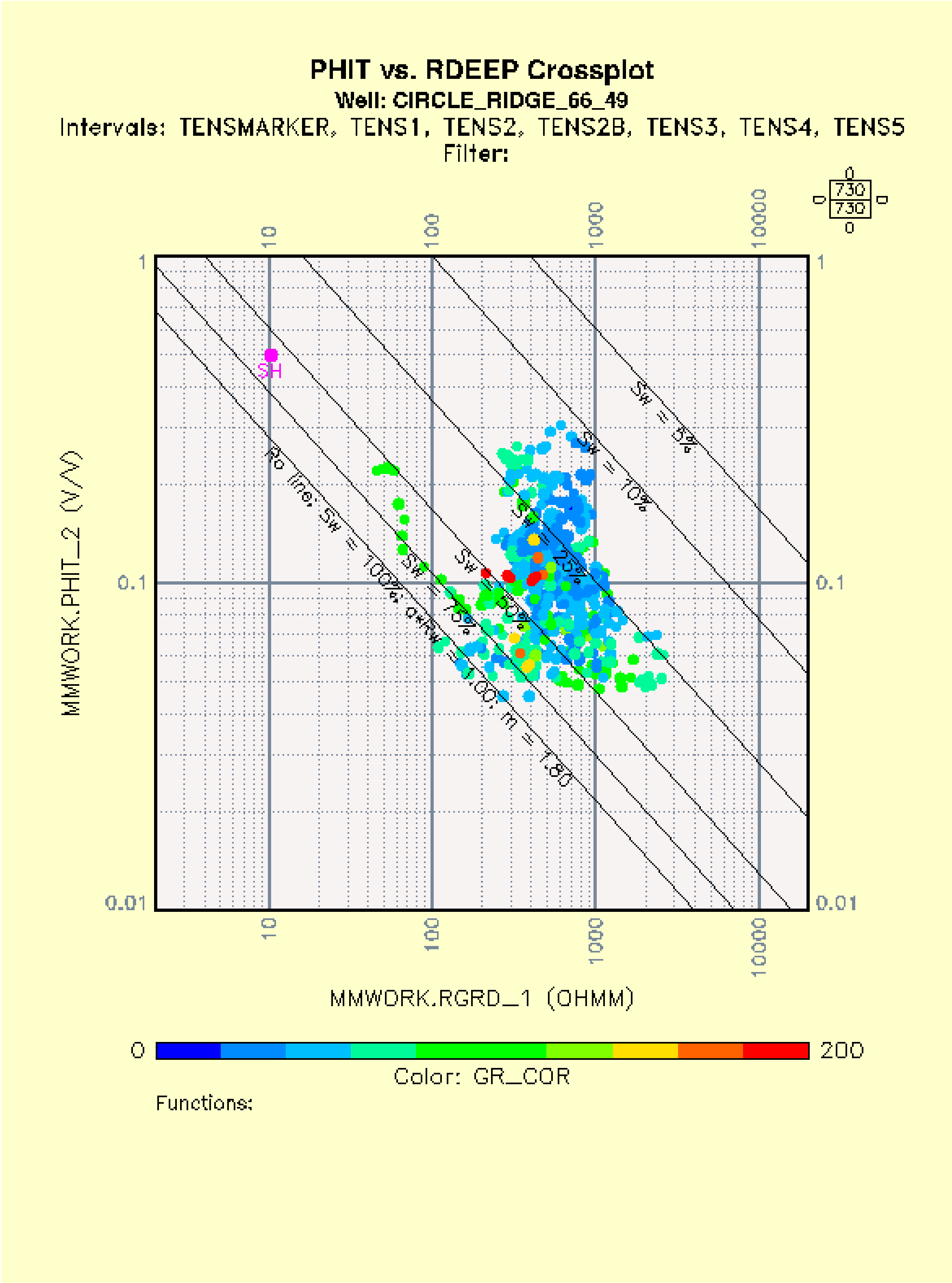


Figure 2-6. Tensleep MULTIMIN predicted and real logs

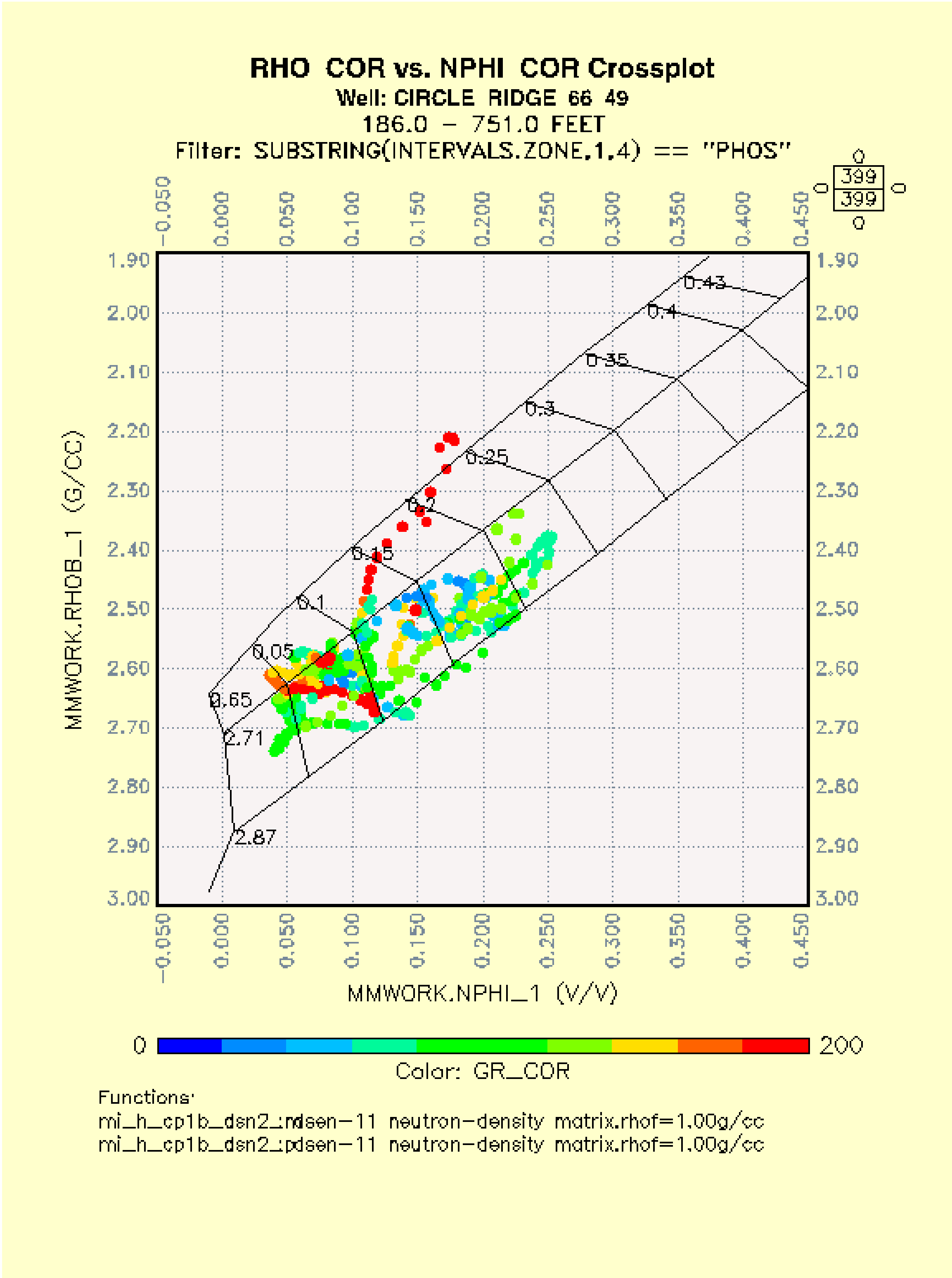


Figure 2-7. Crossplot of rhob and nphi in well 66 49, Phosphoria Formation

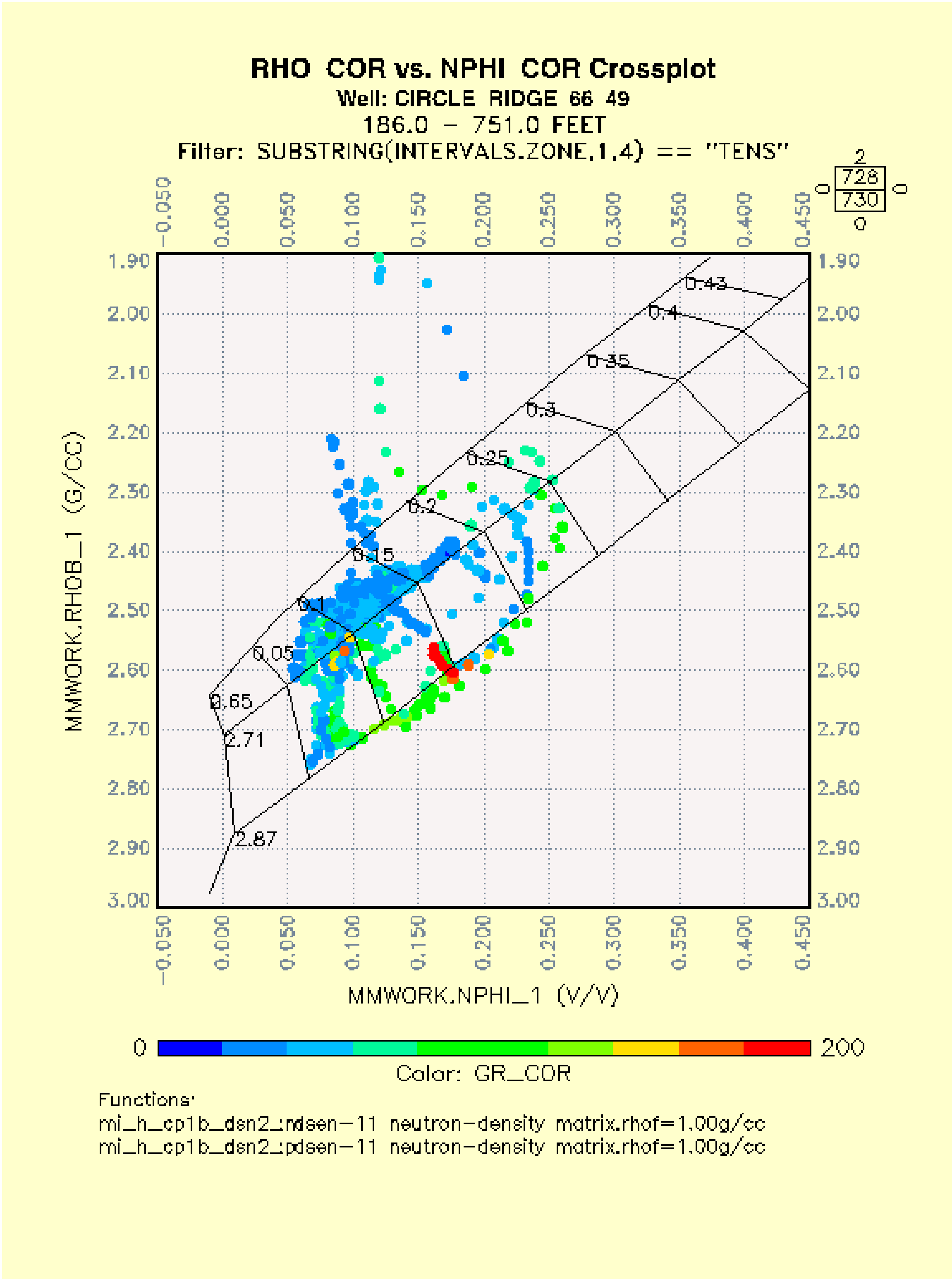


Figure 2-8. Crossplot of rhob and nphi in well 66 49, Tensleep Formation

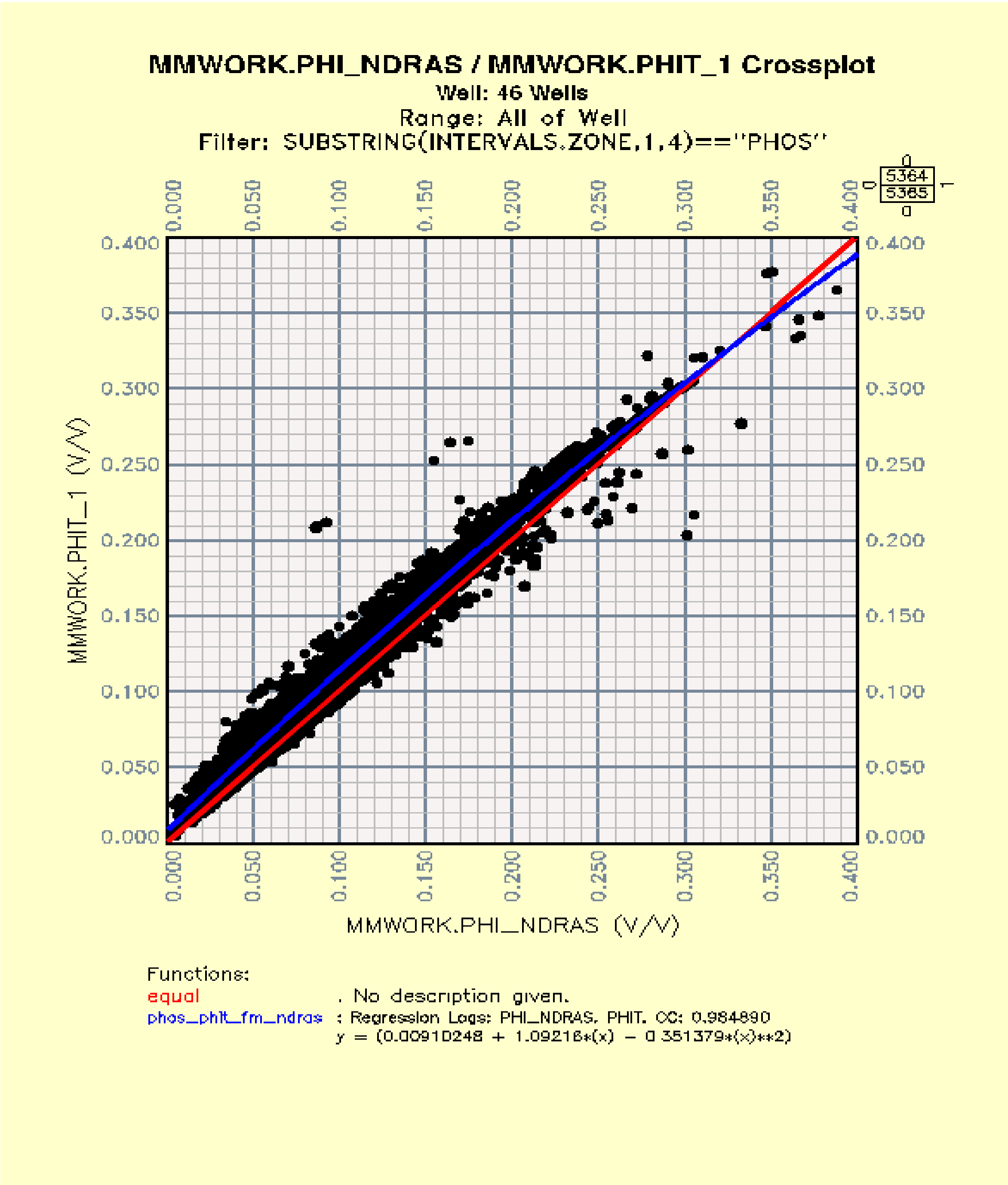


Figure 2-9. Comparison of crossplot porosity (X-axis) to MULTIMIN porosity (PHIT – Y-axis) in the Phosphoria Formation for 46 wells.

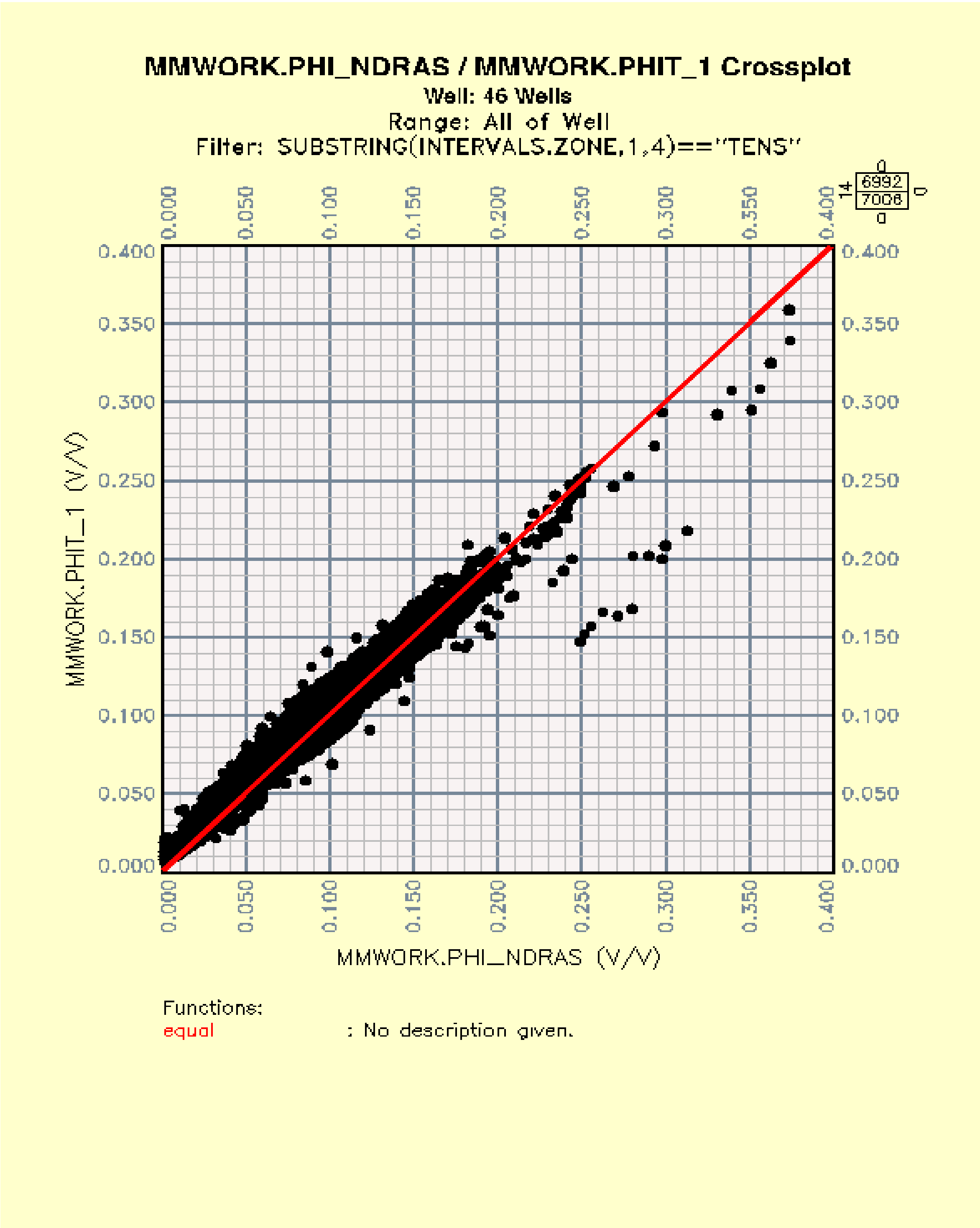


Figure 2-10. Comparison of crossplot porosity (X-axis) to MULTIMIN porosity (PHIT – Y-axis) in the Tensleep Formation for 46 wells.

Track 1: blue - calculated water saturation black - gr
Track 2: depth in feet
Track 3: black - density porosity magenta - MULTIMIN porosity blue - density log

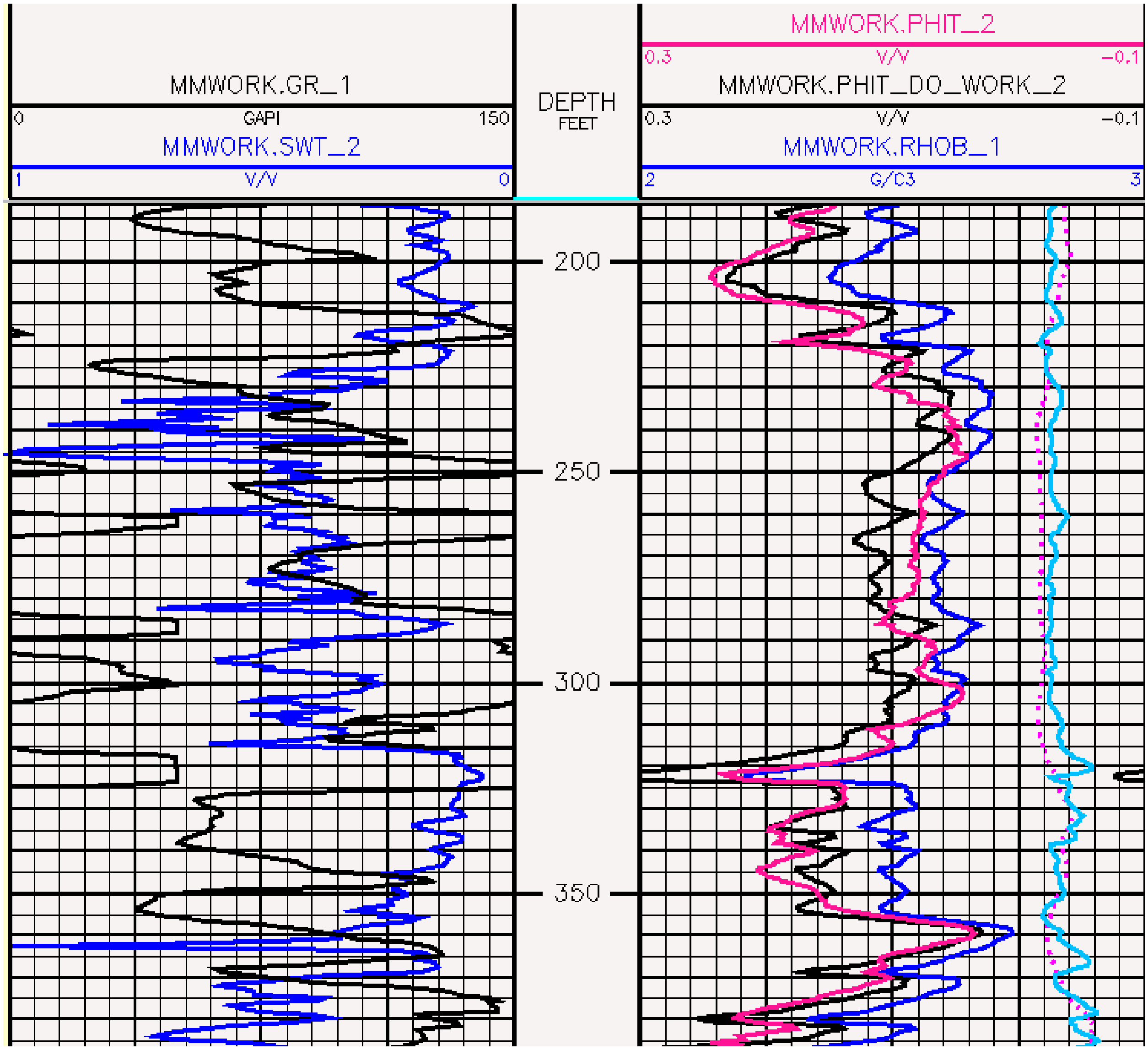


Figure 2-11. Porosity determination from density log, Well 66 49, Phosphoria Formation.

Track 1: blue - calculated water saturation    black - gr
Track 2: depth in feet
Track 3: black - density porosity    magenta - MULTIMIN porosity    blue - density log

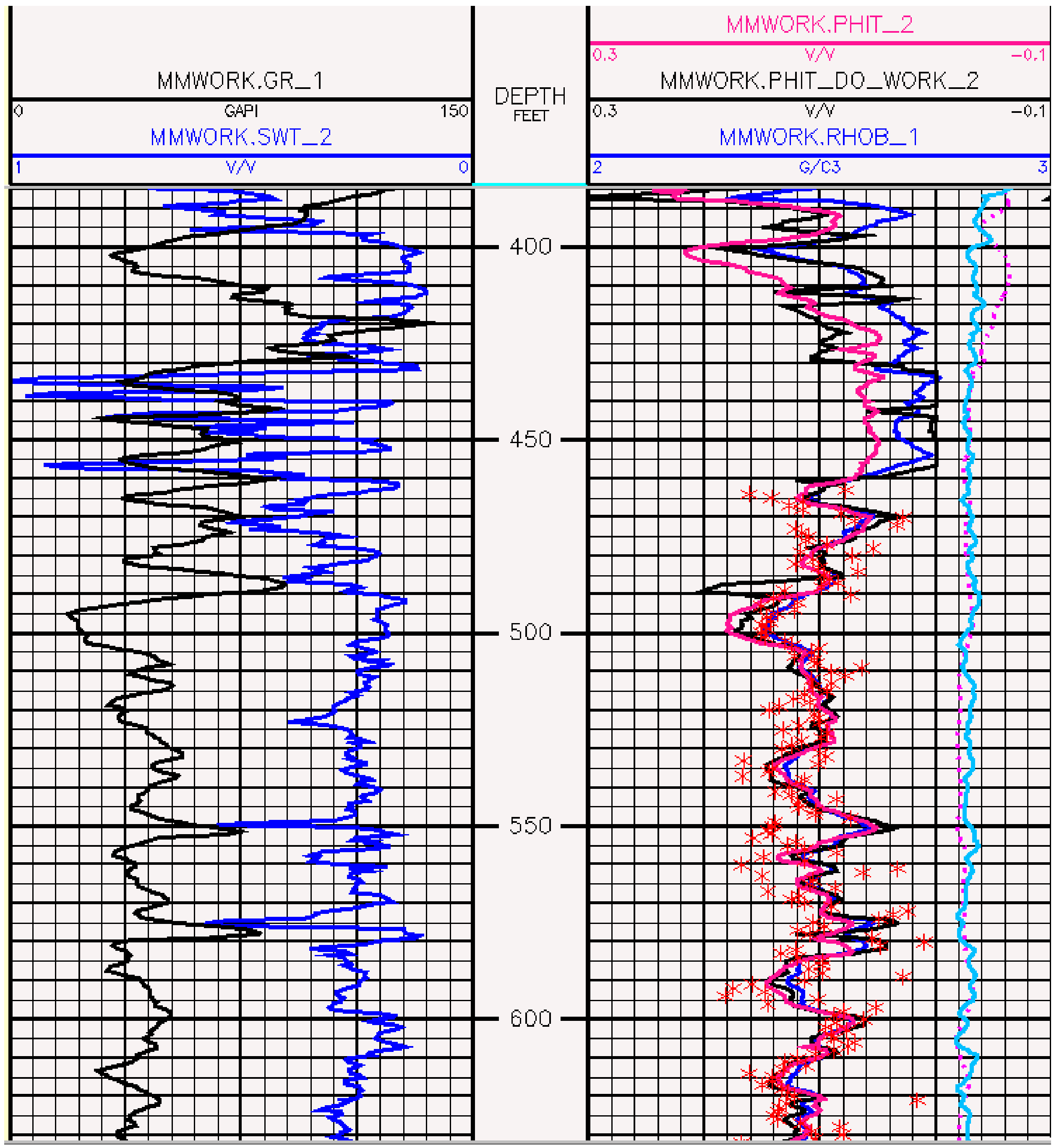


Figure 2-12.    Porosity determination from density log, Well 66-49, Tensleep Formation.

### 2.2.4 DENSITY LOG ONLY

In some wells, density logs are the only porosity logs available, making accurate determination of total porosity more difficult. The method relies upon use of the gamma ray log in concert with the density log to first determine rock type, and then to compute porosity based upon relations and parameter values for the rock type. A solution for each formation was generated, and a LOGLAN (GeoLog® programming language) program was built to handle both the Phosphoria and Tensleep at once. The annotated LOGLAN program is presented in Appendix 6.1.

Figure 2-11 shows the results of the program on well 66-49 Phosphoria Formation. There is reasonable agreement with the MULTIMIN porosity. Figure 2-12 shows the results on the same well in the Tensleep Formation.

This type of analysis was carried out on twenty-three wells in the overthrust and ten wells in the subthrust. No single well of this type contained both overthrust and subthrust sections.

### 2.2.5 GAMMA RAY NEUTRON (GRN) POROSITY

The method used for these wells relies on an old technique of log analysis (Asquith and Gibson, 1982). The wells in the Circle Ridge Field that have only the GRN logs were drilled in the 1950's and 1960's. Of all of these wells, two also contained density logs, which proved very useful for calibration.

Figure 2-13 through 2-15 show the calibration of the GRN using the control provided by the density log for the Tensleep Formation in two wells and for the Phosphoria Formation in one well. The logs for these two wells suggest that it may be possible to estimate porosity from GRN count rate. Near the bottom of the Phosphoria there are anhydrite layers, which produce a low GRN porosity point (or high GRN count rate). The Phosphoria layers "PHOS1" and "PHOS2" shown on the figure generally have higher porosity points (or lower GRN count rates). These observations can be used to estimate porosity in the following manner by re-scaling the transforming a linear count rate (NEU) to a logarithmic porosity value (PHIT_NEU). :

Compute a GRN count rate frequency histogram for the two formations. Figure 2-16 shows this histogram for Well 66-34. This is one of the oldest wells, where the count rate is extremely low. The minimum and maximum values from this histogram are used to define the limits of the input log, in this case, the GRN count (Figure 2-17). In order to map the GRN count rate to the same scale as the porosity, and because of the inverse relation between porosity and GRN count rate, the old minimum value of 1.8 is mapped to 30% porosity, while the old maximum GRN count rate value of 13.2 is mapped to 1% porosity.

Track 1: black - gr log blue - calculated water saturation (SWT) from density porosity
Track 2: depth
Track 3: formation tops
Track 4: magenta - density porosity black - GRN porosity blue - density correction

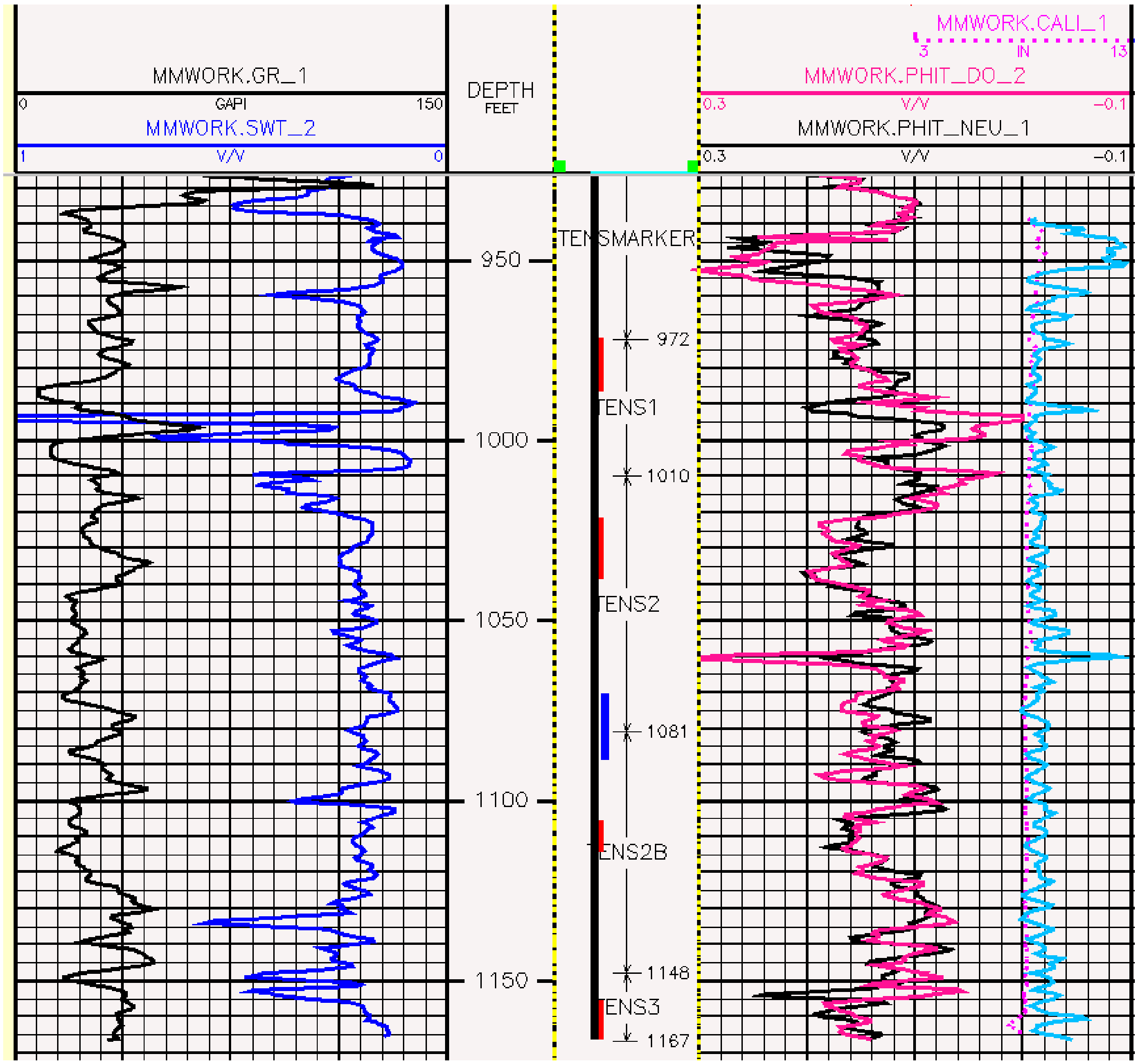


Figure 2-13. GRN log, Well 66 15, Tensleep Formation

Track 1: black - gr log blue - calculated water saturation (SWT) from density porosity
Track 2: depth
Track 3: formation tops
Track 4: magenta - density porosity black - GRN porosity blue - density correction

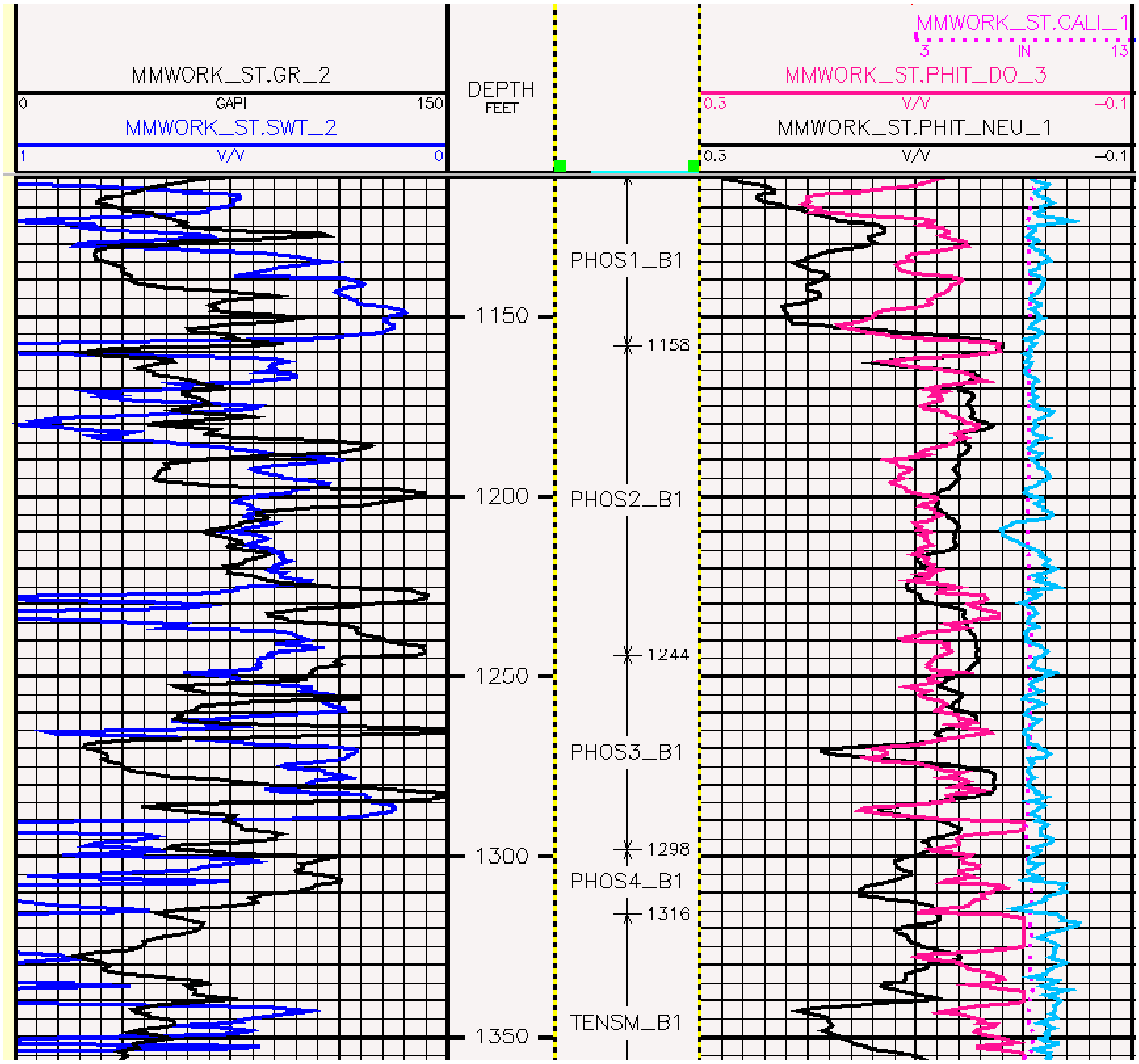


Figure 2-14. GRN log, Well 66 45, Phosphoria Formation

Track 1: black - gr log blue - calculated water saturation (SWT) from density porosity
Track 2: depth
Track 3: formation tops
Track 4: magenta - density porosity black - GRN porosity blue - density correction

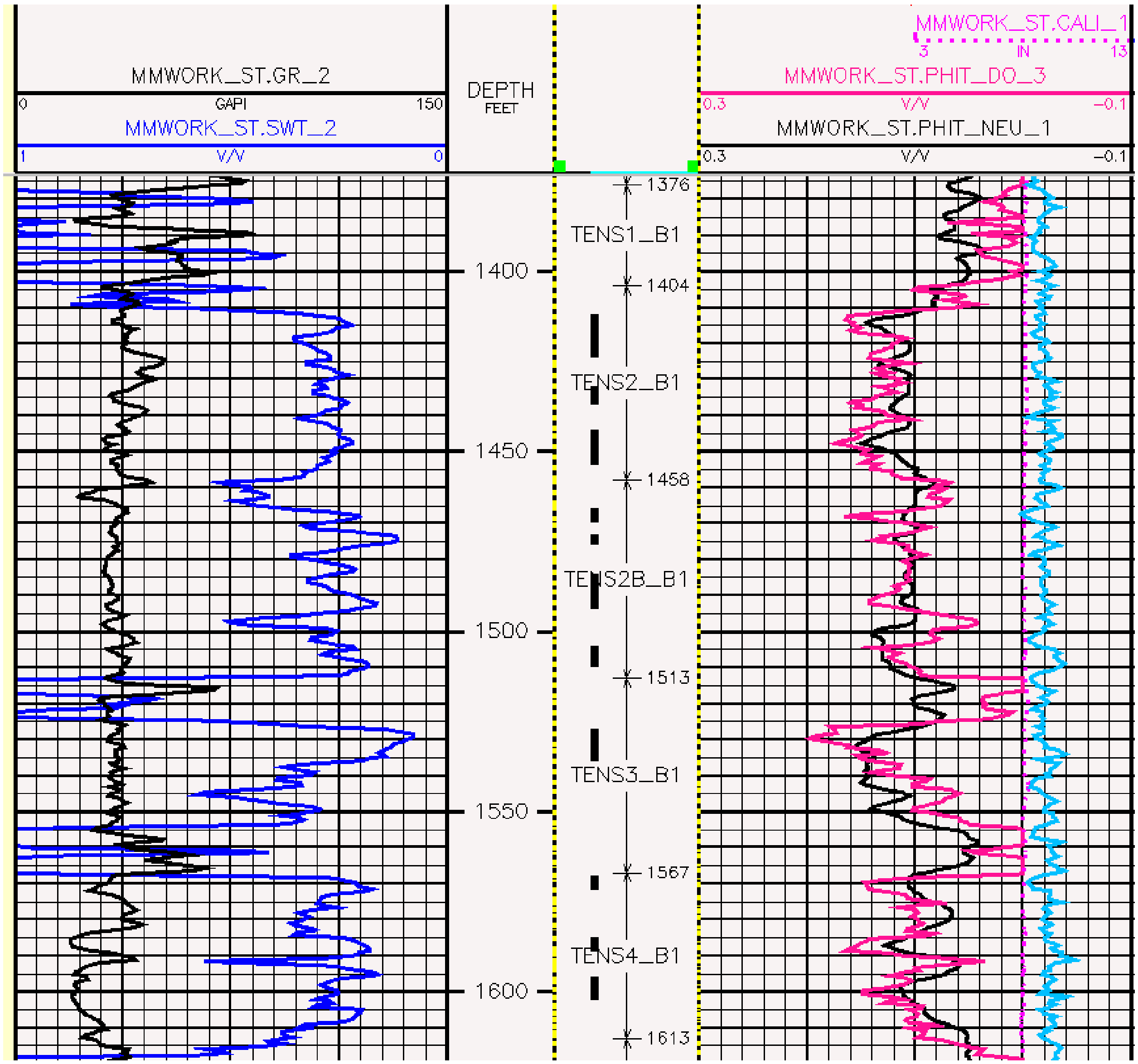


Figure 2-15. GRN log, Well 66 45, Tensleep Formation

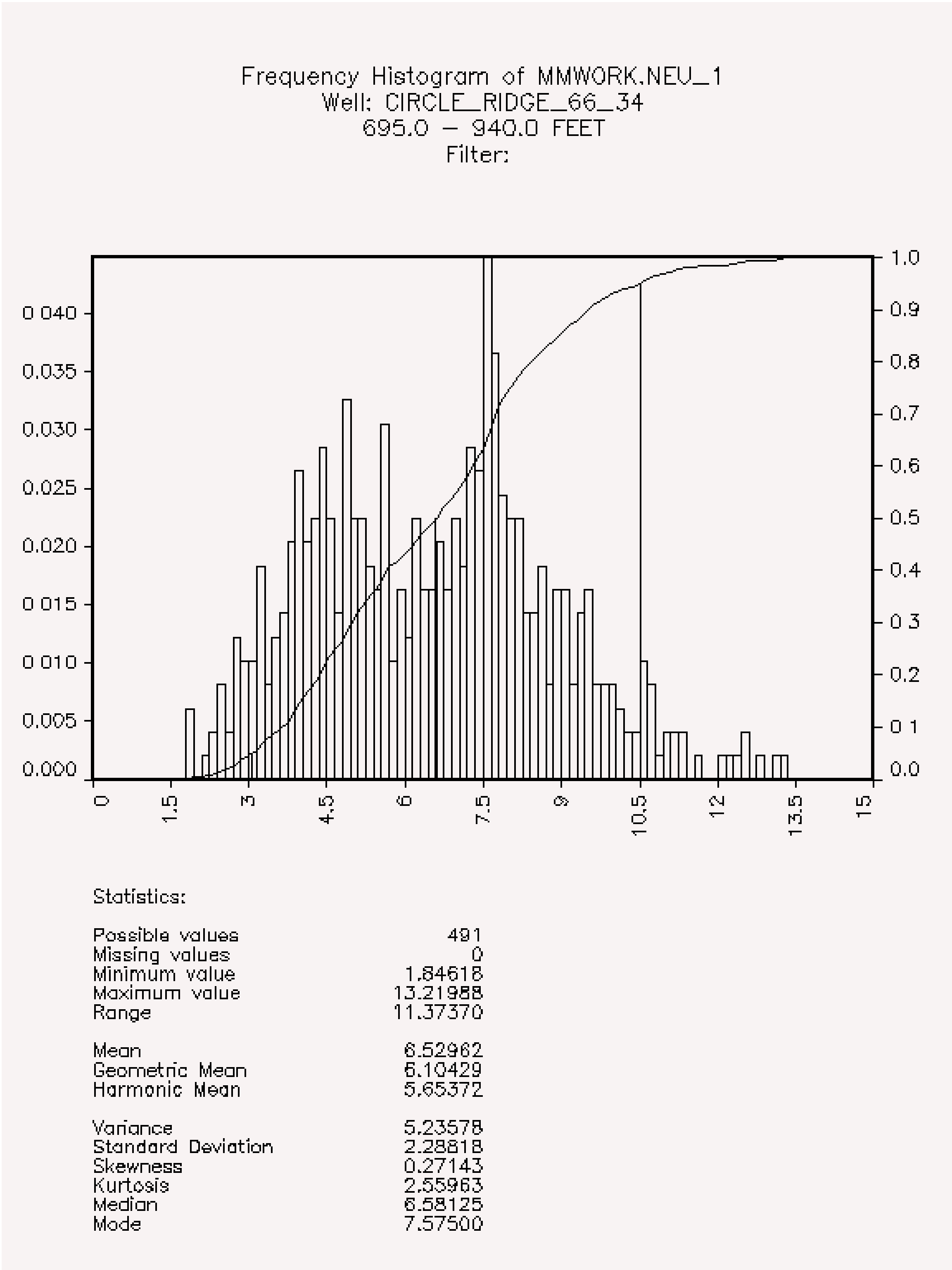


Figure 2-16. Frequency plot of GRN count rate (NEU), Well 66 34

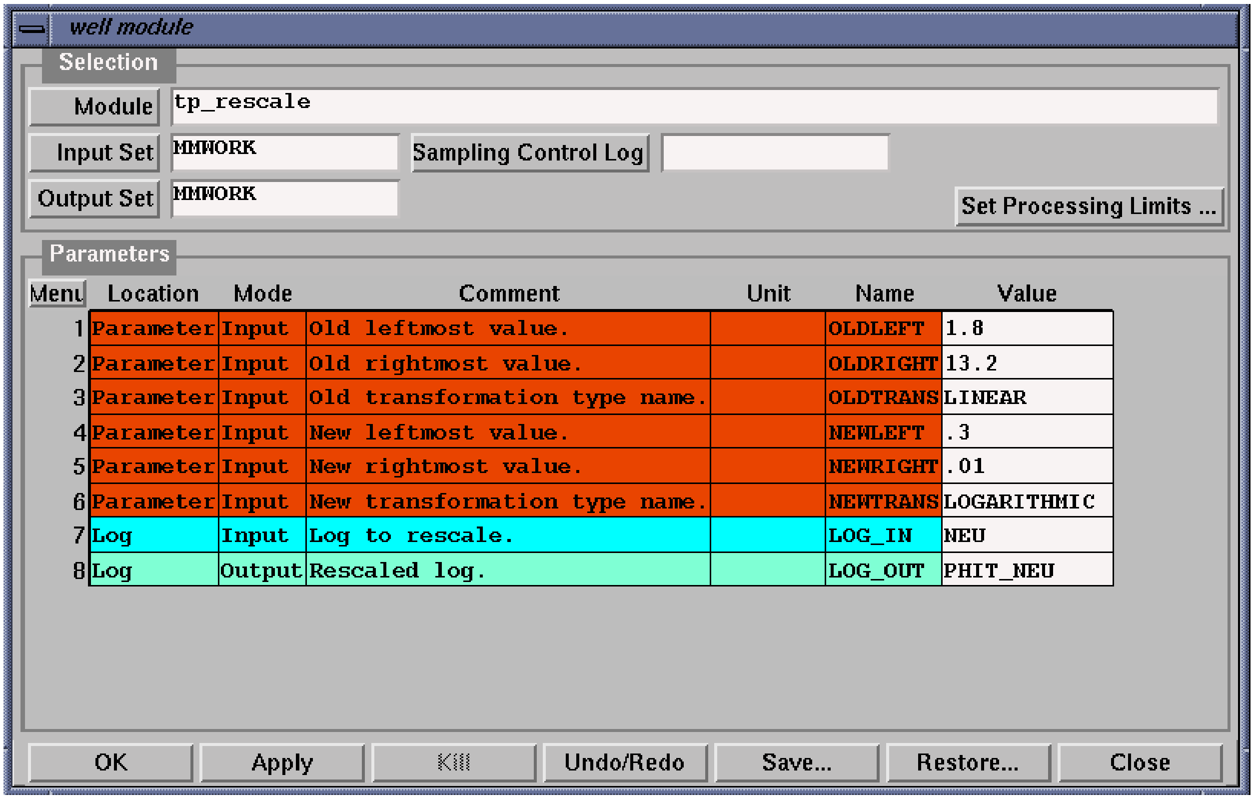


Figure 2-17. Rescale module with representative settings for the GRN count rate (NEU) to porosity (PHIT_NEU), Well 66 34.

### 2.2.6 PLANS FOR NEXT 6-MONTH PERIOD

The analysis work is complete. In addition to beginning to prepare the data for importation into the 3D reservoir visualization of the matrix, the data concerning lithology and porosity will be integrated with the fracture data from the image logs and core to evaluate possible relations between these parameters and fracture development.

## *2.3 Task 2.1 – Compilation of Existing Data*

The existing data in the field consists of some very preliminary attempts to reconstruct the structure of the field, geological mapping of the surface outcrops, and some geological data inferred from well logs. Although not for immediate use in active tasks, there also exists engineering data from a number of wells that will be used to later build and calibrate the discrete fracture network (DFN) model for the Circle Ridge Field under Task 2.6 – Generation of the DFN model, and Task 3.1 – DFN model flow validation.

### 2.3.1 GEOLOGICAL DATA

There have been two previous attempts to construct cross-sections of the Circle Ridge Field. The first attempt was by Anderson and O'Connell (1993), who published two cross-sections through the Field and interpreted the tectonic evolution of the Field based on these reconstructions. Later Smith (2000) remapped the surface geology of the Circle Ridge Field. He combined these maps with Anderson and O'Connell's cross-sections to create a structurally balanced model that was used for computing reservoir volumes, and to look for untested fault blocks.

For this project, Anderson and O'Connell's two cross-sections were digitized and imported into the 3DMove® software (Midland Valley Ltd.) used in this project to carry out the three-dimensional palinspastic reconstruction (Task 2.4). In addition, Smith's (2000) 3D model, visualized in Earth Vision® (Dynamic Graphics, Inc.), was also imported into 3DMove®.

While tops information existed for some wells in the Field prior to this project, a comprehensive tops database was compiled from the existing data and the results of the petrophysical work. The tops database consists of 1296 tops in 184 wells. The location of 6 major faults was also identified and recorded in 78 of these wells, giving 107 control points for these faults in the subsurface.

In order to integrate this well information into the 3DMove® model, it was also necessary to have information on well trajectories. The well path file for 207 wells, including those with tops or fault penetration information, was provided by Marathon Oil Company.

### 2.3.2 WELL TEST DATA

Marathon Oil carried out two interference tests. Each test used an observation well and four offset wells. The first test had well 66-38 as its observation well, and wells 63-5, 63-33, 65-65 and 63-8 as the offset wells. The second test had well 66-50 as the observation well, and wells 66-6, 66-7, 66-11 and 66-12 as the offset wells. Figure 2-18 shows the test results for these two tests.

Several parameters have been inferred by Marathon engineers from these tests. Their interpretations are summarized in
Table 2-1.

The results from these two wells in the central portion of the field show consistent, strong effective permeability anisotropy to the north-northwest. This direction is not parallel to the Field axis, which is more northwesterly at these locations.

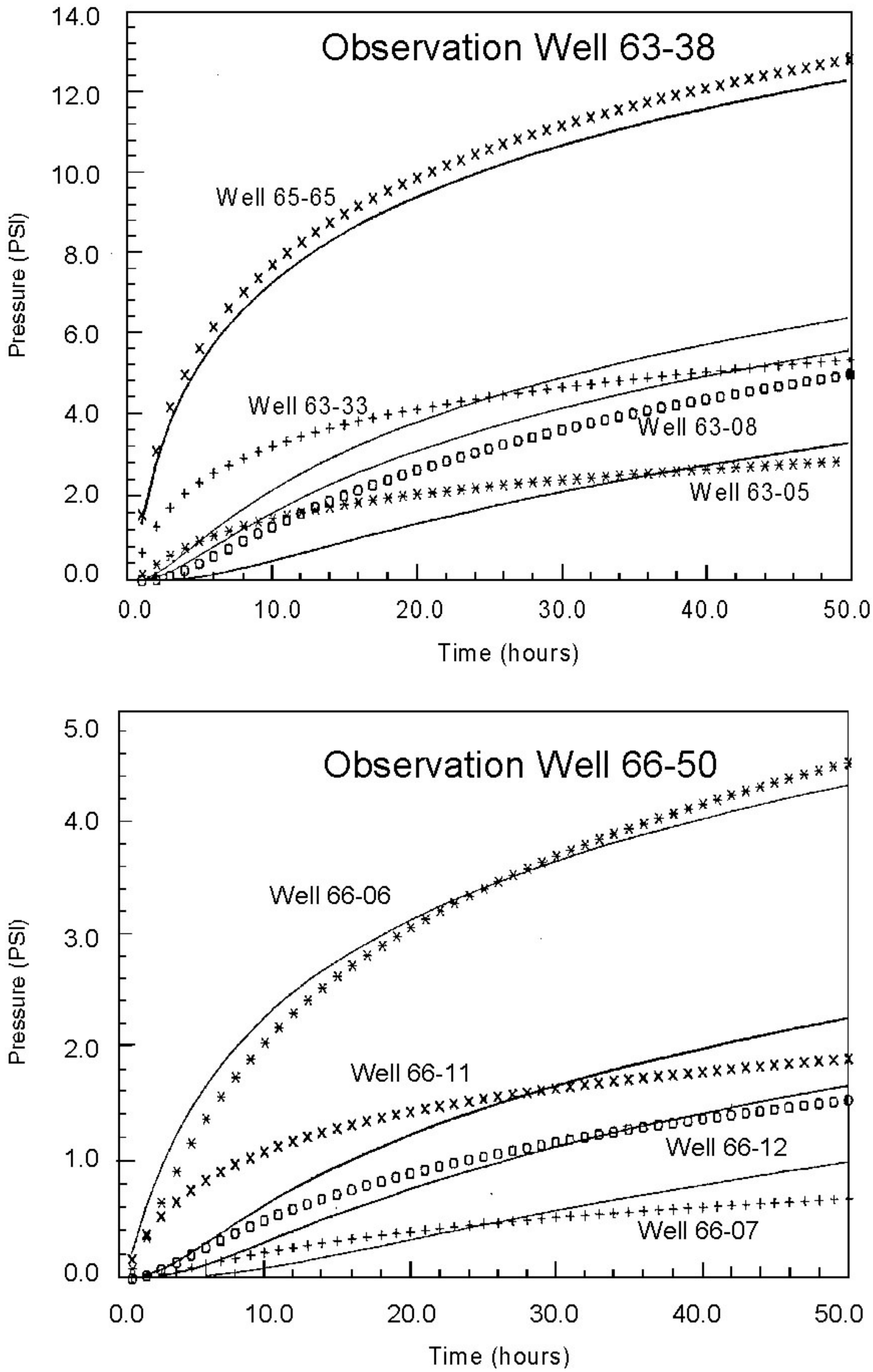


Figure 2-18. Circle Ridge interference tests.

| Observation Well | $K_{max}$ | $K_{min}$ | Theta | Ratio of Maximum to Minimum Effective Permeability |
|---|---|---|---|---|
| 66-50 | 1550. | 20.65 | 282° | 75:1 |
| 63-38 | 700.6 | 8.169 | 286° | 85.7:1 |

Table 2-1. Interpretations of interference tests.

2.3.3 PLANS FOR NEXT 6-MONTH PERIOD

Marathon Oil has provided substantially all of the existing data to the project.

## *2.4 Task 2.2 – Core/FMI/Data Analysis*

Marathon Oil has one core from the Circle Ridge Field. This core is from well 65-48, which is located in the center of the Field. An example portion of the core is shown in Figure 2-19. This core extends from 1130 feet (344.4 m) MD to 1441 feet (439.2 m). This core, described by Marathon Oil geologist B. Curran, contains information on lithology, structures, oil staining, fracturing and other geological information. This core is being used to determine typical fracture styles in the reservoir units, and may be used to provide quantitative fracture geometry information if the existing and future image log data, supplemented by outcrop data, prove insufficient. The spinner and temperature log data has been analyzed to estimate the amount of production contributed by various intervals. Figure 2-20 and Figure 2-21 summarize these results. These graphs show that a large portion of the production comes from a five-foot interval centered around a measured depth of 764 feet (232.9 m).

Marathon Oil will acquire two similar additional data suites from existing open hole completions once the palinspastic reconstructions have progressed to the point that the most useful locations can be identified.

Marathon Oil has also collected new data from well 66-07 over the interval from 722 feet (220.1 m) MD to 974 feet (296.9 m) MD as part of this project. This data includes:

1. FMI image log data;
2. Spinner log data; and
3. Temperature log data.

To date, the image log data has been interpreted by Marathon personnel and includes picks of fractures, classification as to whether they are completely open, partially open, lithologically limited, are resistive or partially resistive. Also identified are bedding, deformation bands, drilling induced fractures, borehole breakouts and any erosional surfaces.


Figure 2-19. Core photograph from well 65-48, core interval 1267 ft (386.2 m) to 1282 (390.8 m) ft MD.

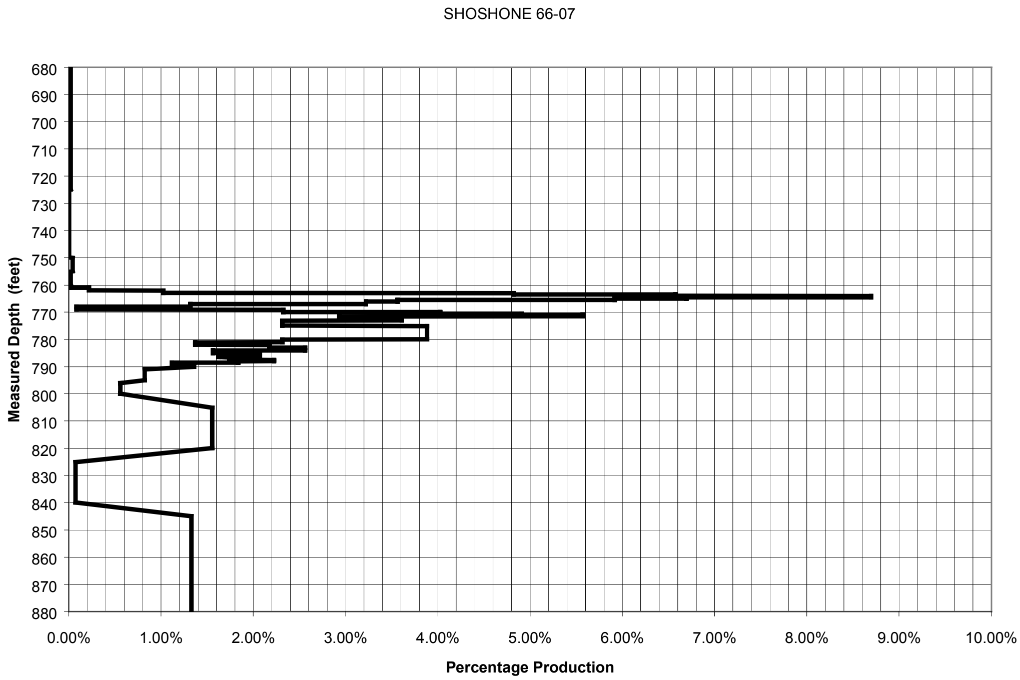


Figure 2-20. Percentage production for intervals in Shoshone 66-07 derived from spinner and temperature log data.

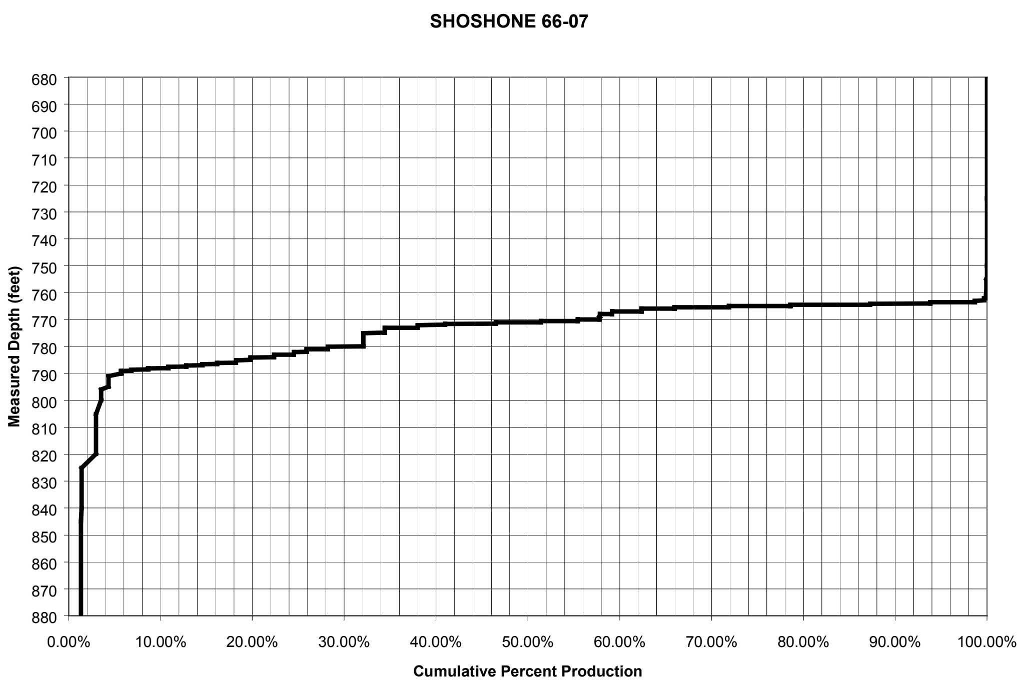


Figure 2-21. Cumulative percentage production for intervals in Shoshone 66-07 derived from spinner and temperature log data.

### 2.4.1 PLANS FOR NEXT 6-MONTH PERIOD

Marathon Oil continues to provide production and other types of well data to the project. During the next six months, it is anticipated that Marathon will provide data on some recently conducted nitrogen injection tests and their interpretation, and acquire FMI, spinner and temperature logs for two additional wells. Also during this period, analysis of the fracture information derived from the image logs, production logs and core will be integrated with the petrophysical data to help develop a geological model for the observed fracturing.

## *2.5 Task 2.3 – Field Data Collection*

Several weeks of fieldwork took place in June and July to gather geological transect data for building cross-sections through the field, and to garner detailed fracture attribute information for key formations and structural positions in order to relate the structural evolution to fracture development.

### 2.5.1 GEOLOGICAL RECONNAISSANCE

Several days of geological reconnaissance were undertaken prior to siting cross-sections and scanlines in order to determine the most useful locations. The starting point for the reconnaissance was the geological map prepared by Smith (2000). The goal was to field check the mapped geology and structure, to update existing or map new faults and folds exposed at the surface, and to determine which formation or formations had fracture patterns that would be most similar to those developed in the reservoir formations, had exposures in several different structural positions, had good fracture development, and also were accessible.

Key findings of the fieldwork were:

1) Smith's (2000) map of geological contacts is sufficiently reliable that his map can be used for constraining the surface geology;
2) The Red Gully Fault, the major fault in the Field, map continue as Smith's Green Valley Fault, and not to the northwest as Smith has mapped;
3) The Orange Canyon Fault and the Blue Draw Fault may have different surface trace locations than mapped by Smith, and may actually be connected by means of a detachment in the Gypsum Springs Formation;
4) The Gypsum Springs Formation is very susceptible to shear along bedding. It forms a major detachment surface in the field. An example of the lack of bedding cohesion in the Gypsum Springs can be seen in T7N, R3W (Figure 2-22). This photograph, looking at some of the steeply dipping beds exposed near the Orange Canyon Fault,

shows how easily the beds can slip and deform. Above the Gypsum Springs Formation in the northwest end of the structure, the overlying Sundance and Morrison Formations are tightly folded into a series of synclines and anticlines while the Gypsum Springs and older units are only involved in much more broad field-scale folding reflected by the outcrop pattern (Figure 2-26) as the structure plunges.

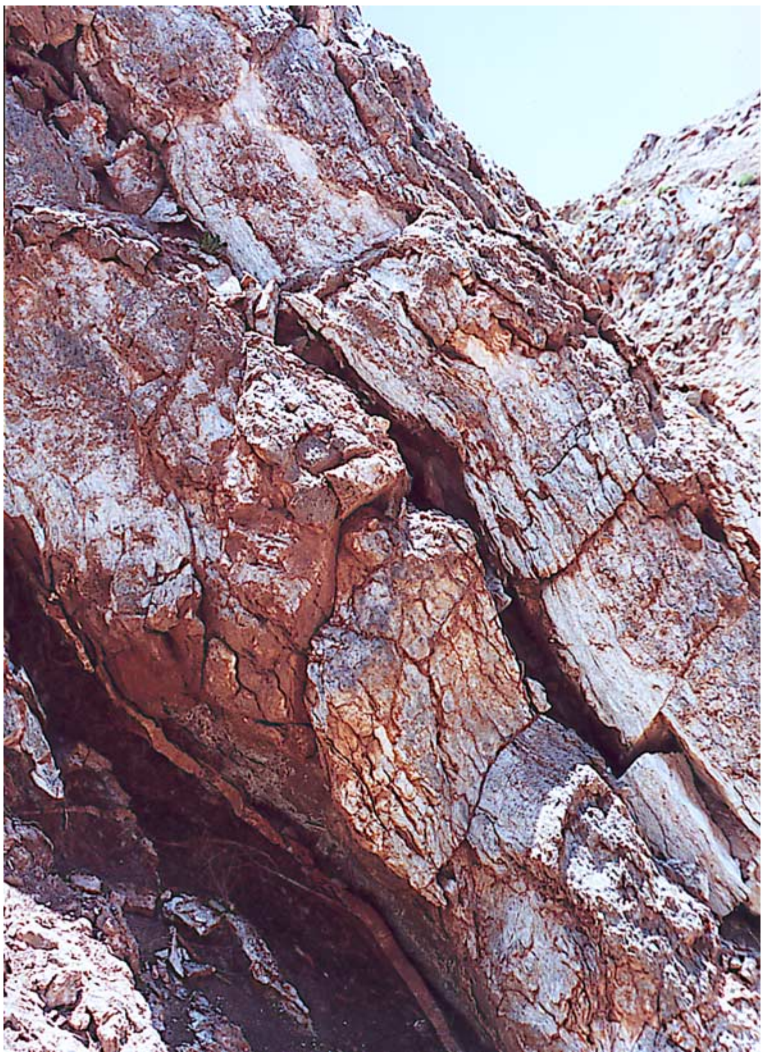

Figure 2-22 Detachments along bedding are common in the Gypsum Springs Formation in the northwest end of the Field. The overlying Sundance Formation near this outcrop is tightly folded into a series of synclines and anticlines, while the underlying Popo Agie and Crow Mountain only show the broad, large-scale folding associated with the Red Gully Fault propagation fold.

Three new cross-sections are being constructed to supplement two existing cross-sections. The locations of these sections were devised to provide constraints on critical portions of the field. Their locations are shown in Figure 2-23.

Two of the new cross-sections were located in the northwestern end of the Field. This is an area of considerable structural complexity where there are several major faults and the hinge of the fold changes azimuth.

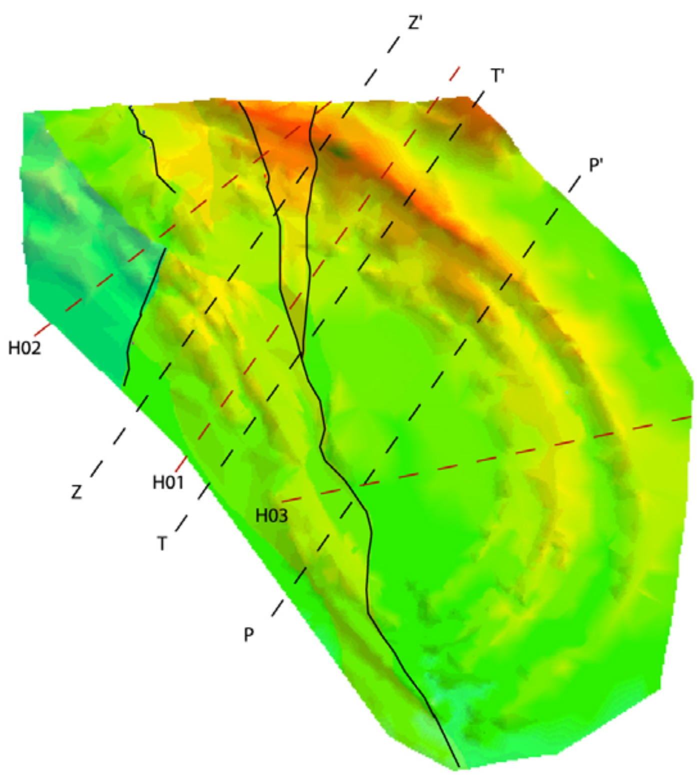


Figure 2-23. Picture showing the topography of Circle Ridge. The spectrum corresponds to elevation where red is the highest and green represents the lower parts. The fault traces of the Red Gully and Green Valley faults cross cut the whole field. Orange Canyon and Blue Draw are also shown in the NW part of the field. The cross-sections are shown as hatched lines. The P, T and Z sections were produced by Anderson and O'Connell (1993) and H01, H02 and H03 are the new cross-sections from the June field campaign.

### 2.5.2 ACQUISITION OF OUTCROP FRACTURE DATA FROM SCANLINES

Fracture data was measured along eleven scanlines located in the Red Peak and Crow Mountain units. These units were selected since they are below the Gypsum Springs (see legend in Figure 2-26), had fracture patterns that were reasonably well developed, and had reasonably accessible outcrops in a variety of structural positions throughout the

Field. Scanline data acquisition requires information on the geometry of the scanline in order to carry out various types of bias corrections (La Pointe and Hudson, 1985). Each scanline consisted of one or more *legs*, which are segments of the line that are well-approximated by a straight line. The use of legs is necessary if the outcrop face departs from planarity at the scale of the scanline. The relative position along the scanline tape, which leg it belonged to, its orientation, trace length, termination style, sense of movement (if discernable), and additional comments were recorded for each fracture intersecting the tape or whose projection would intersect the tape. Information was obtained in this way for a total of 541 fractures – 290 in the Crow Mountain Formation and 251 in the Red Peak Member.

Appendix 6.2 contains all of the data obtained along these eleven scanlines.

### 2.5.3 PLANS FOR NEXT 6-MONTH PERIOD

No additional fieldwork is planned for the next six-month period.

## *2.6 Task 2.4 – Construction of Balanced Cross-Sections*

To understand where fractures form in a geologically complex environment, rock units can be unfolded and restored back to their original unfolded and unfaulted flat lying depositional position. Forward restoration from this initial configuration makes it possible to estimate the strains developed during the process. By using the 2D or preferably 3D strains from a successful restoration process across the field, fractures can be generated in accordance with the matching strain model. Moreover, restoration provides better geometrical definition of the fault block architecture of the reservoir which is crucial for maximizing cost-effective and technically efficient recovery.

The geological development of an oilfield often involves several deformation mechanisms such as compressional folding, thrusting, fault propagation folds, and so on. Each type of deformation requires a specific type of restoration mechanism such as flexural slip, fault parallel flow or shear strain, often in combination with each other. In order to unravel the complex deformation history, it is necessary to understand the current geological situation well. In the case of the Circle Ridge Field, this requires a good 3D geological model over the field before any attempt to perform any restoration process begins.

Table 2-2 shows the input data used for constructing a 3D geological model over the Circle Ridge field.

| Input data | Description | Performed by |
|---|---|---|
| Field data | Field data with explicit mapping of faults and fractures. | Performed by the project team in June 2000. |
| Cross-sections | 3 sections across the field in approximately NE-SW direction (P-P', T-T' and Z-Z') | Anderson and O'Connell (1993) |
| | 3 additional sections, two in NE-SW direction and on E-W (H01, H02, H03) | Performed by the project team in June 2000 |
| Well data | Formation tops from 206 wells drilled across the field | Marathon Oil |
| | 115 reanalyzed wells with reinterpreted formation tops | Performed by the project team in August 2000 |
| Geological model | 3D EarthVision model over the field | Smith (2000) as part of a BSc degree at The Baylor University, Texas |

Table 2-2. Data sources for palinspastic reconstruction of Circle Ridge Field.

Additional information was taken from Anderson and O'Connell (1993) and from Marathon Oil geologists Brendan Curran and Ken Steele, and engineers Mike Dunleavy, Jim Baker.

The geological model exactly follows the well formation top data from the two separate data sets available (see Table 2-2). The formation tops interpreted by the recent analysis by Straub (GeoData Services; see Section 2.2) prevails when differences occur between the two data sets. The cross-sections performed by Anderson and O'Connell (1993; Figure 2-23and Figure 2-24) have been used to control the shape and the offset of faults and horizons. However, these cross-sections are traced from published papers and do not contain relevant coordinate data which excludes them for being a direct part of the 3D geolgical model. On the other hand, the newly aquired cross-sections H01, H02 and H03, shown in Figure 2-25, are included in the 3D model and provides good control of the extension of the formations up to the surface. Note that the locations of the recently aquired cross-sections have been recorded with GPS measurements which is essential when incorporating the data into a 3D model. Finally, the model have been conditioned to the geological outcrop map presented by Anderson and O'Connell (1993) and Smith (2000; see Figure 2-26).

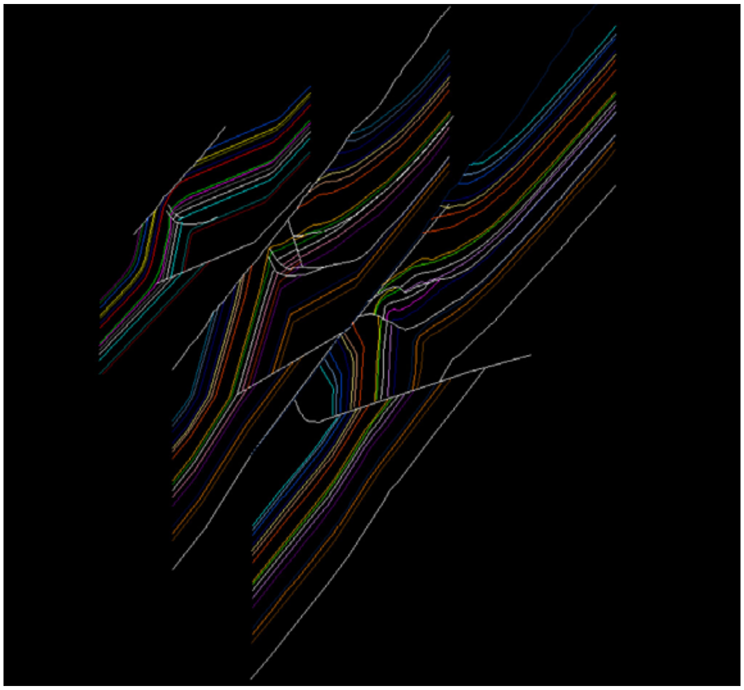

Figure 2-24. Perspective view of the Anderson and O'Connell (1993) P, T ad Z sections as they appear in the 3D model.

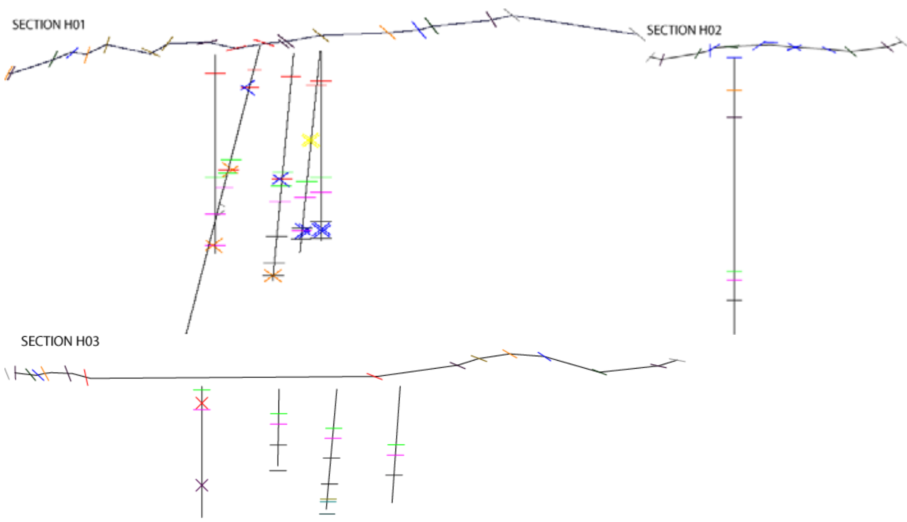


Figure 2-25. Cross-sections H01, H02 and H03 performed by the project team during the June 2000 field campaign.

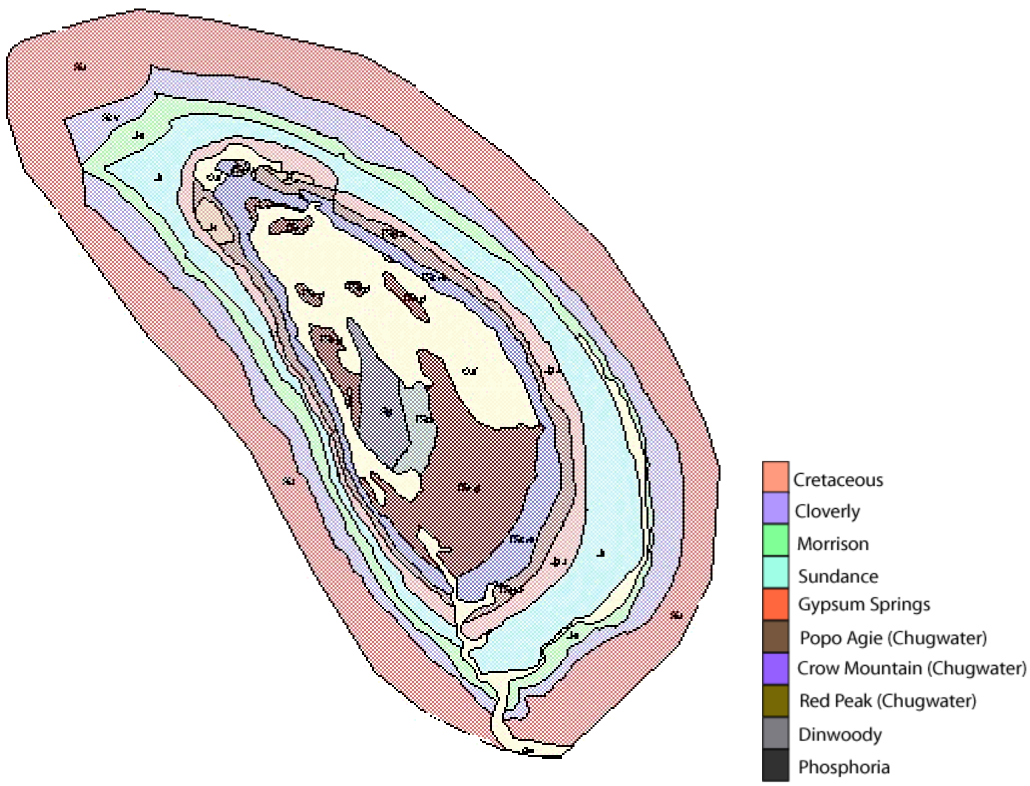


Figure 2-26. Geological map of Circle Ridge modified after Anderson and O'Connell (1993) and Smith (2000).

Circle Ridge's structure is well expressed in the surface topography as seen in Figure 2-23. Prominent cuestas clearly define the "kidney-shaped" structure from air photos and are therefore excellent markers for field mapping. The Circle Ridge anticline has been erosionally breached, and thus forms a topographic basin in the center. The main anticline axis trends N 15º-20º W, nearly perpendicular to the N 40º-50º E stress direction inferred as the principle direction of horizontal compression during the Laramide Orogeny. The fold is overturned, with the steepest beds on the southwestern flank. Resistant limestone beds of the Jurassic Sundance Formation forms vertical standing walls, such as the one shown in Figure 2-27.

A fault-propagation fold is the best interpretation for the overall structure of Circle Ridge (Anderson and O'Connell, 1993). Fault-propagation folds form when a master propagating thrust fault loses slip and terminates upsection. Observations supporting a fault-propagation interpretation at Circle Ridge include the fold asymmetry and the southwestern overturned limb. However, the controlling reverse fault has not yet been identified, presumably because it lies beneath any current well penetrations. Seismic data in the area are too poor in quality to identify such a fault with any confidence.

Several smaller, northeast dipping, thrust faults imbricate the crest of the structure. The number of reverse fault imbrications, as identified from borehole data, increases in the northwestern part of the field. The Red Gully Fault (RGF), the fault with greatest amount

Figure 2-27. Competent sandstone horizons in the Sundance Formation forms vertical walls of rock in the southern part of Circle Ridge.

of displacement at Circle Ridge, cuts the field into two blocks termed the overthrust block (Figure 2-28) and the subthrust block. The subthrust block (footwall block of the Red Gully Fault) actually consists of several sub-blocks divided by the Blue Draw Fault (BDF), Gray Wash Fault (GWF), Purple Sage Fault (PSF), and Yellow Flats Fault (YFF) that compartmentalize the reservoirs (Figure 2-29). The Blue Draw Fault, like the Red Gully Fault, has surface exposure while the others are recognized only from well data. One of the major concerns of the geological model is the extension of these faults in the subthrust block. Several imbrications possibly exist between the Green Valley Fault and the Red Gully fault making the northeasterly part of the field extremely complex.

The palinspastic reconstruction is performed in 3D space restoring key formations back to the undeformed state. As the collected fracture data comes mainly from the Red Peak and the Crow Mountain formations they will be used as controlling horizons and will be the main focus for strain together with the producing units Phosphoria and Tensleep. The complete geological model contains data for all horizons down to the Darby formation and are listed in Figure 2-28 and also shown in Figure 2-30.

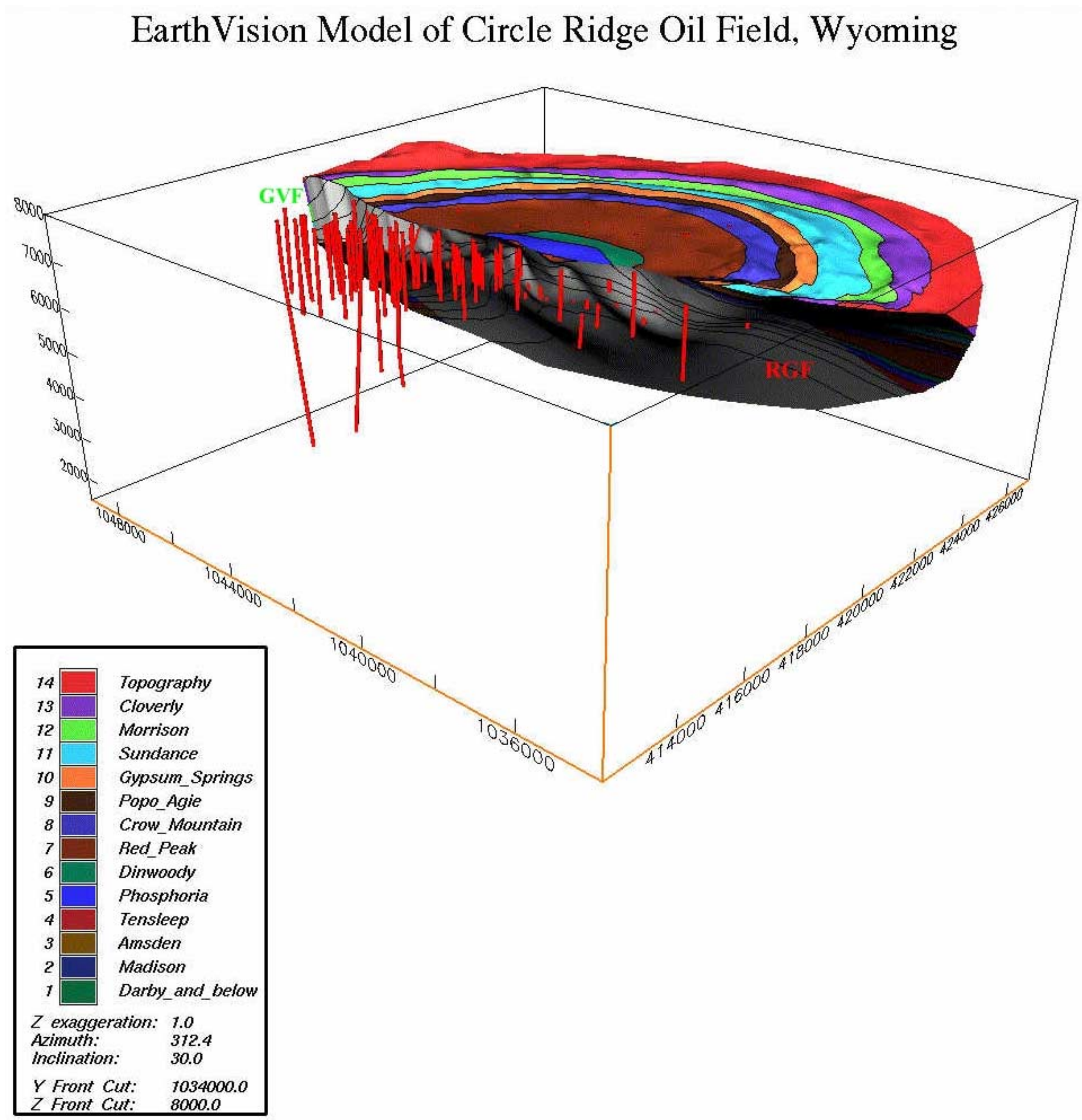


Figure 2-28 Overthrust block at Circle Ridge after Smith (2000).

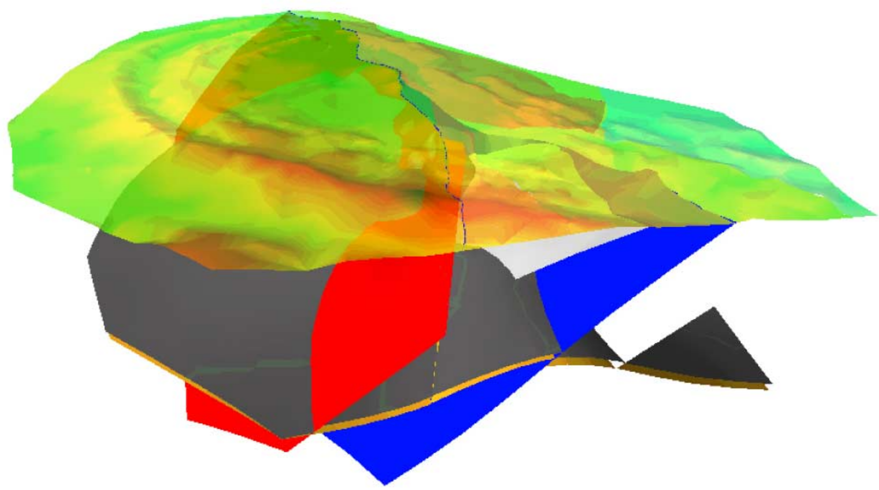

Figure 2-29. 3D Model of the major faults in the field; The Red Gully (red) and Green Valley (green) Faults and the Blue Draw Fault (blue), Gray Wash Fault (gray), Purple Sage Fault (behind), and Yellow Flats Fault (behind) together with the Phosphoria (gray) and Tensleep (orange) formations.

The dominating strain mechanism to restore Circle Ridge is interpreted to be fault parallel flow along the main Red Gully thrust. However, the smaller fault blocks in the northern part of the field may well be better explained by other restoration mechanisms such as parallel shear and flexural slip.

The restoration process was begun in October, but is not scheduled to be completed until early in 2001.

### 2.6.1 PLANS FOR THE NEXT 6-MONTH PERIOD

It is anticipated that the 3D palinspastic reconstruction will be completed over the next six months.

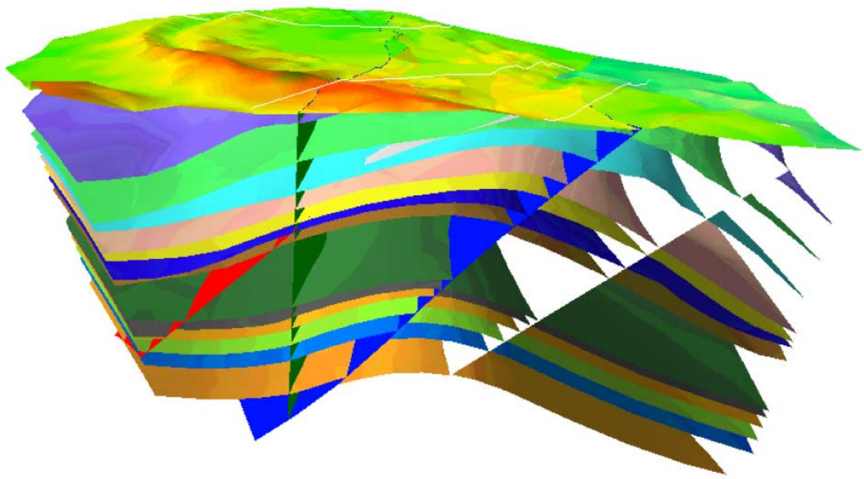

Figure 2-30. Perspective view of the complete geological model of the Circle Ridge Field. For a color legend, see Figure 2-28.

## *2.7 Task 5.1 – Project Web Site*

### 2.7.1 WEB SITE DEVELOPMENT

In an effort to provide new and innovative ways to communicate project results to interested persons and organizations, an interactive web site has been. The web site contains general information about the project, data and data analysis results, and links to other related sites on the World Wide Web. Figure 2-31 shows the homepage of the Circle Ridge web site, which can be found at http://www.fracturedreservoirs.com.

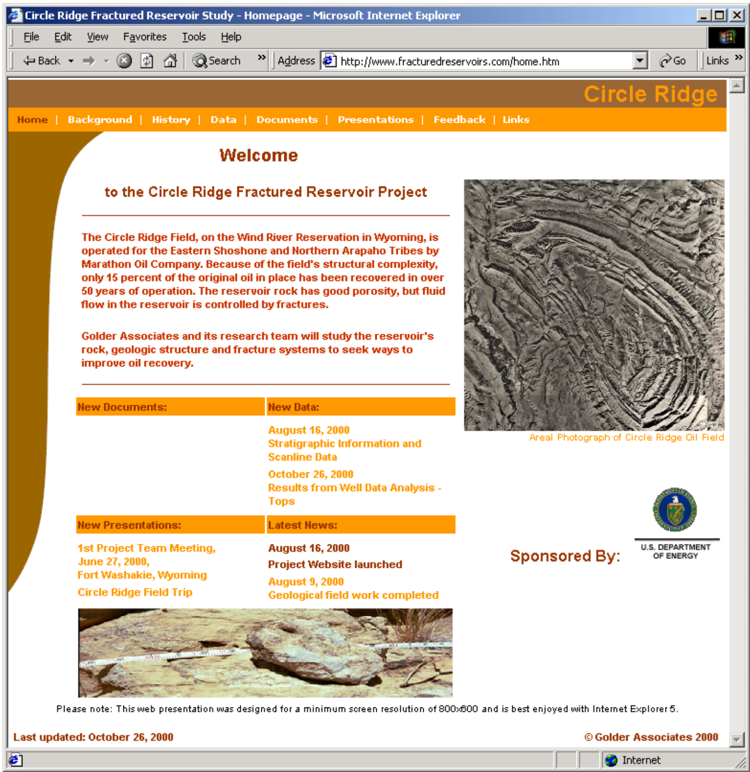


Figure 2-31 Homepage of Circle Ridge Website

The contents of the web site are divided into the following sections:

| | |
|---|---|
| Background | General information about the Circle Ridge project |
| History | Brief description of the history of the Circle Ridge Oil Field |
| Data | Project Data Warehouse |
| Documents | Progress Reports and Papers related to the Circle Ridge project |
| Presentations | Presentations given during the Circle Ridge project |
| Feedback | Form to provide feedback to the project team |
| Links | Links to related sites on the World Wide Web |

The heart of the web site is the interactive, dynamic data warehouse. The warehouse uses an air photo of the Circle Ridge Oil Field in combination with different maps (geological map, well locations) to provide an intuitive and easy way to navigate to the data of interest. Users can select which map is projected on top of the air photograph (see Figure 2-32) and then click on a point on the map or on a list on the right side of the photo to display the associated data:

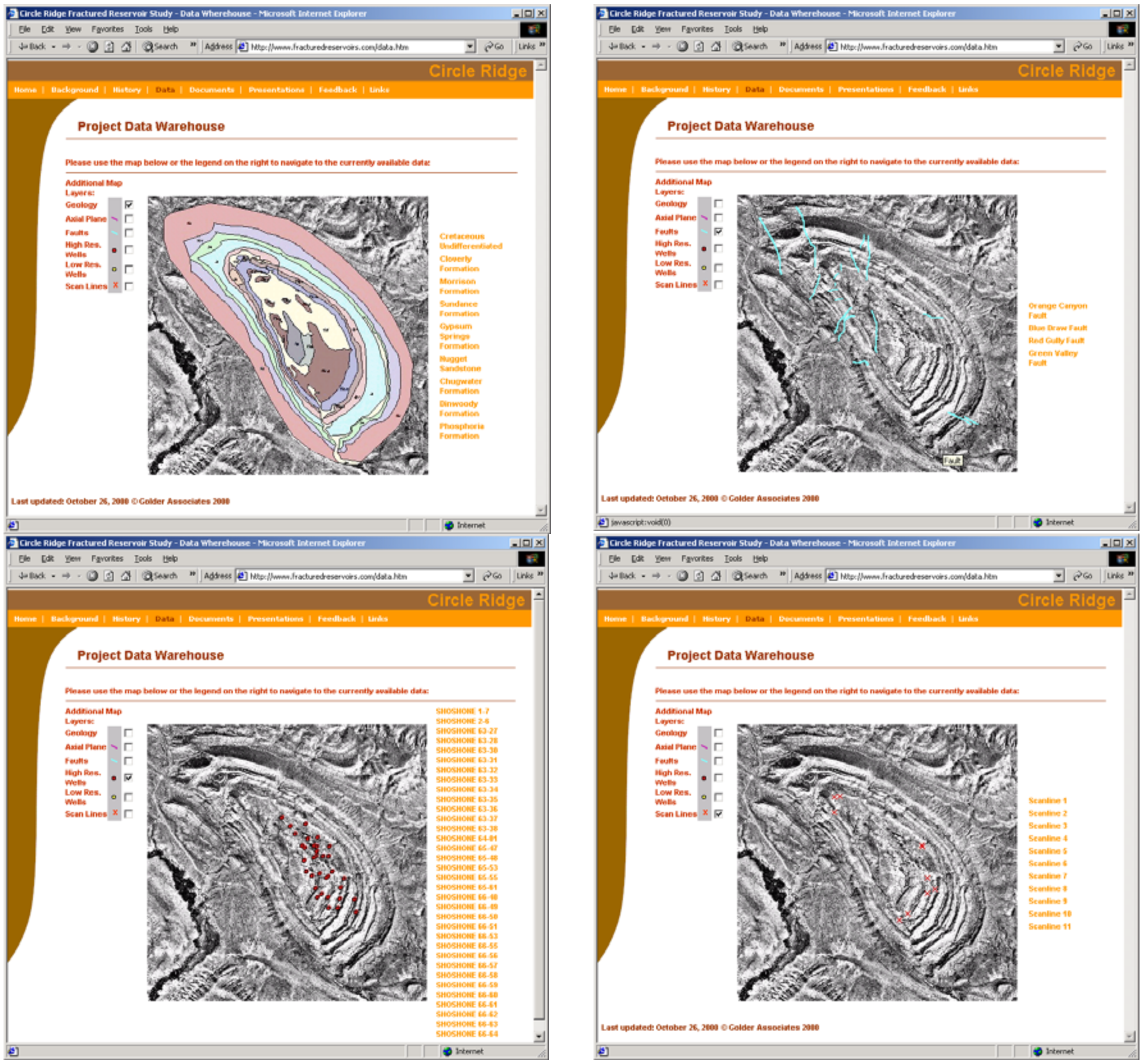


Figure 2-32 Project Data Warehouse

The following data is currently available through the data warehouse:

- Location and description of the most important geological formations
- Location of the axial plane of the Circle Ridge structure
- Location of major faults and description of four of those faults
- Location of 34 wells with high-resolution data. Tops of reservoir formations in those wells.
- Location of 166 wells with low-resolution data. Tops of reservoir formations in those wells.
- Location of 11 scanlines taken during the June 2000 field trip. Fracture data along each of those scanlines.

### 2.7.2 WEB SITE STATISTICS

Since the web site was launched on August 16, 2000, it was visited 164 times. 62 of those visits were made by first time visitors, 102 visits were repeat visits.
The site currently has a size of 4.66 MB (pages, data, pictures) and contains 331 individual web pages.

### 2.7.3 PLANS FOR THE NEXT 6-MONTH PERIOD

The next feature to be added to the web site will be a 3-D model of the structure of the Field. The model can be rotated, panned, zoomed, etc., allowing the user to investigate the details of the structure of the field. A prototype has been developed that is composed of an initial reconstruction of the present-day structure. This type of display will serve as a visualization mechanism for the 3-D palinspastic reconstruction results, allowing the user to examine the structure at different times in its evolution.

In addition, results from the analysis of fracturing along scanlines and its relation to the structural evolution will be posted.

Additional data from wells will be posted as it becomes available.

A copy of this report will also be made available through the web site.

## *2.8 Task 5.3 – Workshop for Tribes*

The Circle Ridge project constitutes a new beginning in the exploitation of the Circle Ridge Field. Success in this current project, as well as improved exploitation of other fields within the Wind Rover reservation that are similar to the Circle Ridge Field, will benefit from a good understanding among all stakeholders of what the project has accomplished, how the technology can be adapted to other fields, and what sort of results can be expected. The goal of the Workshops is to facilitate this level of understanding among the decision makers within the Tribes, Marathon Oil and other interested parties who are not intimately involved with the project. These meetings provide an opportunity for direct dialog between the project personnel and the stakeholders, to complement the other means of communicating the project results, such as the website and professional presentations, reports and papers.

The first workshop was held on June 27, 2000 in Ft. Washakie, WY. Representatives from the tribal Oil and Gas Commission, other tribal members, the Bureau of Land Management, Marathon Oil, GeoData Services and Golder Associates were in attendance. After a brief introduction to the project by Marcy Woods (Marathon Oil), Paul La Pointe (Golder), Jan Hermanson (Golder) and Roger Straub (GeoData) made a presentation. An electronic portion of this presentation may be viewed or downloaded from the project website at http://www.fracturedreservoirs.com. In addition to the material contained in this electronic presentation, GeoData Services displayed preliminary petrophysical interpretation results of the type described in Section 2.2 of this report. In order to further widen the exposure of the project, Marathon Oil distributed the electronic version of the presentation to the following individuals, some of whom were not able to attend the meeting:

Mr. Richard Burnett
Mr. Chester Pingree
Mr. John Enos
Shoshone Oil and Gas Commission

Mr. Anthony Addison, Sr., Chairman
Northern Arapaho Business Council

Mr. John Washakie, Chairman
Eastern Shoshone Business Council

Mr. Stuart Cervoski
U. S. Dept. of the Interior
Bureau of Land management, Lander Resource Area Office

Mr. Larry Murray
Director EDA
Eastern Shoshone Tribe Planning Department

Mr. Mike Lawson
Minerals Director
Northern Arapaho Tribe

John Schumacher, Esq.
Law Office of John Schumacher.

During the workshop, we were pleased to learn that an enrolled member of the Northern Arapaho tribe, Sherry Blackburn, also an intern with Marathon Oil, was available to assist us with some of the fieldwork. She assisted in the field with measuring fractures along scanlines (as detailed in the Geological Fieldwork slide show contained in the project web site), and also with completing the third cross-section.

### 2.8.1 PLANS FOR THE NEXT 6-MONTH PERIOD

No workshops with the Tribes are scheduled for the next six-month period. However, we expect informal contacts with the Tribes to continue, and to take advantage of any project-related visits to Marathon's Cody, WY office to present interim results to the Tribes if possible.

### 2.8.2 OTHER PLANS NOT RELATED TO NEW TASKS BECOMING ACTIVE IN THE NEXT 6-MONTH PERIOD

The next six month period will focus on completion of the palinspastic reconstruction and completion of the analysis that is required to construct the 3D discrete fracture network models. The later will include analysis of much of the well and field data collected during the first six months from the perspective of how it can be used to determine the parameter values for the model.

# 3 RESULTS AND DISCUSSION

During the first six months of this project, which is primarily a data acquisition phase of the project, there are few final results. The preliminary results for each active first-level task are discussed below.

## 3.1 Task 1 – Petrophysical Analysis

Task 1 focused on the petrographic work to determine matrix properties for a large number of wells that had varied type and quality of logs available for porosity and lithology determination. This work has been completed successfully. 39 wells (one more than originally planned) that had modern logging suites were analyzed in both the overthrust and subthrust portions of the reservoir. The techniques proposed for re-analysis of the more than 113 wells that only had limited or much older vintage logs available also proved successful. Results for these wells have been posted to the project web site, provided as electronic files, and passed on to Marathon personnel for use in building the complete 3D reservoir matrix model (Task 3.2).

## 3.2 Task 2 – Development of Structural Conceptual Model

The main activities for this Task during the first six months have been to acquire all of the necessary field data for use in the 3D palinspastic reconstruction and begin reconstruction, and to acquire new and compile existing outcrop and subsurface fracture data for later creation of the reservoir-scale DFN model of fracturing (Task 2.6).

Several weeks of fieldwork at the Circle Ridge Field accomplished the project goals for Tasks 2.1 and 2.3. Three new transects were completed across the field in critical areas not covered by the two existing cross-sections published by Anderson and O'Connell (1993). In addition to field checking Smith's (2000) geological map, the two existing cross-sections and developing a more complete understanding of the larger-scale structure of the Field, key formations and locations were identified for acquiring outcrop fracture data through scanline mapping. The geological reconnaissance carried out to support the 3D reconstruction showed that the Jurassic Gypsum Springs Formation can form a major detachment horizon in the section. There is particularly excellent field evidence of this decoupling of structure above and below the Gypsum Springs in the northwestern end of the Field. Thus, folds and fracture patterns seen in formations above the Gypsum Springs may not reflect the fracture pattern in formations below, such as the Phosphoria and Tensleep Formations that comprise the two most important reservoir units in the Field. For this reason, fracture data was acquired in scanlines in the Triassic Red Peak Member of the Chugwater Formation. The Red Peak Member is the lowermost formation exposed in Circle Ridge that has outcrops in a variety of structural positions and locations. The locations selected for the scanlines are in both the main overthrust and subthrust fault blocks, and are distributed in both the noses and flanks of this doublylunging anticline. These positions will make it possible to better evaluate the relation between the fracture pattern and structural position.

The initial reconstruction work has indicated that Anderson and O'Connell's (1993) and Smith's (2000) work provide good starting points, but need substantial modifications in order to match the new tops and fault information obtained during the first six months of this project.

# 4 CONCLUSIONS

As the project has focused on data acquisition during the first six months, supplemented with some preliminary analyses, conclusions primarily relate to these issues rather than to the behavior of the reservoir and the development of reservoir management strategies or engineering decisions. The main conclusions of the completed work are as follows:

1. The various strategies employed to estimate values of porosity (and lithology and fluids where data allowed) appear to have been successful. This has resulted in a nearly four-fold increase in the number and representative coverage of matrix properties and formation tops for the reservoir. This increased coverage will directly benefit the accuracy of the model of the matrix properties, the knowledge of matrix controls on fracturing and their use in conditioning the discrete fracture network model, and improve the reliability of the palinspastic reconstruction.
2. Fieldwork and the new cross-sections based on this and existing sections suggest that the broad outlines of previous work (Anderson and O'Connell, 1993; Smith, 2000) are generally correct, but will still require substantial modifications in order to result in a balanced model.
3. The decoupling of the rock above the Gypsum Springs Formation from that below suggests that fracture patterns in rock younger than the Gypsum Springs may have different fracture patterns than in the older rocks, such as the primary reservoir units. For this reason, fracture measurements in the Sundance Formation may be hard to relate to the fracturing in the reservoir, particularly in the northwest and southeast ends of the Field where folding is more intense and outcrops indicate structural decoupling. Fracturing in the Sundance may be less impacted by decoupling in the flanks of the Field where deformation is less and stratal dips are less.
4. Interference tests in the central portion of the Field suggest that the effective reservoir permeability is strongly anisotropic, the direction of greatest permeability slightly to the north of west. This direction is diverges somewhat from the more northwesterly trend of the main fault in the Field for reasons not yet known.

# 5 REFERENCES

Anderson, T. C. and P. J. O'Connell (1993). Strcutral geology of the Circle Ridge Oilfield, Fremont County, Wyoming. Wyoming Geological Association Guidebook, Special Symposium-1993, pp. 399-418.

Asquith. G. and C. Gibson (1982). Basic Well Log Analysis for Geologists. American Association of Petroleum Geologists, Methods in Exploration Series, Tulsa, OK (4th Printing), 216p.

La Pointe, P. R. and J. A. Hudson (1985). Characterization and Interpretation of Rock Mass Joint Patterns. Geological Society of America, Special Paper 199, 37p.

Smith, V. (2000). Surface Geologic Map of the Circle Ridge Oil Field, Wyoming. M. S. Thesis, Baylor University, Waco, TX.

# 6 APPENDICES

## 6.1 Loglan program for density-only wells

```
PROGRAM: PHIT_RHOB  Phit estimate from single porosity wells
with rhob

/*------------------------------------------------------------
-----------------
/*start_doc
/*Rhob in the Phosphoria\Tensleep to Phit estimate.
/*end_doc
/*------------------------------------------------------------
-----------------

INPUT
/*
/* CONSTANTS ----------------------
/*
    GRMT                               /*
    dpthsw                             /* et boundary
/*
/* INTERVALS ----------------------
/*
ZONE                   ALPHA*12  /*
/*
/* LOGS ---------------------------
/*
   RHOB                   G/C3      /* Bulk Density
   GR                     GAPI      /* Gamma Ray
   DEPTH                  FEET      /*

LOCAL
   rhomce                           /* for Phosphoria
   rhomct                           /* for tensleep

OUTPUT
/*
/* CONSTANTS ----------------------
/*
    GRMT                             /*
                                     /*
/* LOGS ---------------------------
/*
    PHIT_DO                v/v /* Total Porosity

START:
```

```
  rhomce = 2.79
  rhomct = 2.77
dowhile GET_FRAME ()
  if (depth<dpthsw) then      /*   if   depth   is   in   the
Phosphoria
     phit_do = (2.79 - rhob)/1.79  /* use straight 2.79 for
matrix
  else                             /* now in the Tensleep
     if (rhob > 2.55 & gr < grmt) | gr > 80 then  /*check GR
& rhob values
     if rhomct < 2.84 then  /*if rhob heavy and gr high
          rhomct = rhomct + .05    /*or low then in dolomite
     endif
     else
     if ( rhomct > 2.67) then /*if  we  don't  meet  the  above
conditions
          rhomct = rhomct - .05    /*then we're in quartz…
          endif
     endif
     phit_do = (rhomct - rhob)/(rhomct - 1)  /*    calculate
our porosity
  endif
        phit_do = limit(phit_do, 0, 1)  /*     limit     the
porosity
        call PUT_FRAME ()          /* save the porosity

enddo
```

## *6.2 Scanline Data*

Scanline data was collected at 11 different sites. The header information indicates the orientation of the scanline, which is defined by one or more legs. A leg is a portion of the scanline that is approximately a straight line. For each fracture, its location along the scanline, which leg it belongs to, its orientation in terms of quadrant strike and dip, its trace length in the scan plane, the type of terminations of each end of the trace, any detectable sense of movement, and additional comments have been recorded. The codes for terminations are as follows:

U = unknown. The fracture trace is not observable
T = terminates at a high angle against another fracture
A = terminate at a low angle or asymptotically against another fracture
H = terminates by hooking into another fracture
B = fracture terminates in the rock matrix

### 6.2.1 SCANLINE 1

| | | | | | | | | | |
|---|---|---|---|---|---|---|---|---|---|
| Scanline Data 070300 | | | | | | | | | |
| Name | SCANLINE_1 | | | | | | | | |
| | | | | | | | | | |
| GPS points along the scan line | | | | | | | | | |
| Waypoint | Altitude | Scanline distance (ft) | | Leg | Orientation | | | | |
| 113 | 7310 | 2 | | | | | | | |
| 114 | 7316 | 18 | | 1 | 114 | -16 | | | |
| 115 | 7340 | 35.5 | | 2 | 70 | -6 | | | |
| 116 | 7350 | 40 | | 3 | 45 | 10 | | | |
| | | | | | | | | | |
| Rocktype | | | Red Peak Siltstone | | | | | | |
| | | | ft | in | | | | | |
| Stratigraphic thickness | | | 6 | 5 | | | | | |
| Bedding orientation | | | N59E | 26N | | | | | |
| | | | | | | | | | |
| DATA | | | | | | | | | |
| **Scanline length** | **Leg** | **Orientation** | | **Trace length** | | **Terminations** | | **Movement** | **Comments** |
| Ft (decimal) | | Strike | Dip | Ft | In | Upper | Lower | | |
| 3.38 | 1 | N6E | 87E | 4 | 6 | T | A | NORMAL | |
| 5.15 | 1 | N15E | 77E | 4 | 5 | T | T | | |
| 5.73 | 1 | N33E | 31N | 4 | 0 | T | U | | |
| 5.67 | 1 | N11W | 83E | 1 | 2 | T | H | | |
| 6.27 | 1 | N10W | 79E | 18 | 0 | U | U | | FAULT |
| 7.04 | 1 | N19E | 77E | 6 | 5 | U | U | | |
| 7.65 | 1 | N4E | 74E | 3 | 9 | A | T | | REDUCTION |
| 7.98 | 1 | N10W | 79E | 2 | 0 | H | B | | REDUCTION |
| 8.74 | 1 | N7W | 81E | 4 | 9 | U | T | | |

| | | | | | | | | | |
|---|---|---|---|---|---|---|---|---|---|
| 9.4 | 1 | N5W | 86E | 1 | 10 | U | T | | |
| 9.77 | 1 | N20E | 85E | 1 | 4 | A | B | | |
| 10.2 | 1 | N16E | 65E | 5 | 10 | U | U | | |
| 13.75 | 1 | N7W | 70E | 2 | 8 | A | T | | |
| 18.98 | 2 | N2W | 89E | 1 | 7 | T | B | | REDUCTION |
| 19.27 | 2 | N0W | 88W | 4 | 9 | U | B | | WIDTH 1.5" |
| 19.34 | 2 | N39E | 84W | 2 | 8.5 | A | A | | REDUCTION |
| 20.55 | 2 | N11E | 88E | 5 | 3 | U | U | ? | FAULT |
| 20.88 | 2 | N66E | 78S | 6 | 0.75 | A | U | | |
| 22.05 | 2 | N14E | 71E | 4 | 2 | T | A | | |
| 22.8 | 2 | N32E | 78W | 3 | 9 | A | U | | |
| 22.58 | 2 | N35E | 85N | 3 | 4 | U | A | | |
| 25.7 | 2 | N59W | 72S | 6 | 9 | U | U | | WIDTH 1" |
| 26.18 | 2 | N12E | 61E | 5 | 11 | U | U | | WIDTH 1" |
| 26.77 | 2 | N31E | 59S | 6 | 1 | U | U | | |
| 29.63 | 2 | N30E | 58S | 4 | 5 | U | A | | |
| 31.36 | 2 | N44W | 74W | 3 | 7 | T | U | | |
| 30.15 | 2 | N39E | 73S | 5 | 8 | U | U | | WIDTH 2.5" |
| 31.21 | 2 | N40E | 74S | 10 | 0.5 | A | A | | |
| 31.3 | 2 | N33E | 81S | 2 | 2 | T | A | | |
| 31.6 | 2 | N32E | 65S | 2 | 8 | U | U | | WIDTH 3" |
| 32.2 | 2 | N23E | 63E | 5 | 9 | U | U | | |
| 32.9 | 2 | N21E | 55E | 5 | 9 | U | U | | |
| 35.4 | 2 | N47E | 67W | 12 | 2 | U | U | | WIDTH 1" |
| 37.35 | 3 | N64W | 77W | 3 | 10 | A | U | | |
| 37.5 | 3 | N66W | 74S | 12 | 2 | U | U | | |
| 38.35 | 3 | N5E | 65E | 4 | 1 | U | T | | |
| 38.7 | 3 | N32W | 85W | 2 | 3 | A | U | | |
| 39 | 3 | N82W | 78S | 1 | 9 | U | A | | |
| 39.02 | 3 | N29E | 65E | 2 | 6 | U | U | | |
| 40.2 | 3 | N5E | 59E | 4 | 3 | U | U | | |
| 40.7 | 3 | N7E | 62E | 1 | 2 | T | A | | |

### 6.2.2 SCANLINE 2

| | | | | | | | | | |
|---|---|---|---|---|---|---|---|---|---|
| Scanline Data | 070300 | | | | | | | | |
| Name | SCANLINE_2 | | | | | | | | |
| | | | | | | | | | |
| GPS points along the scan line | | | | | | | | | |
| Waypoint | Altitude | Scanline distance (ft) | | Leg | Orientation | | | | |
| 117 | 7365 | 1 | | | | | | | |
| 118 | 7351 | 16 | | 1 | 130 | -26 | | | |
| 119 | 7349 | 26 | | 2 | 68 | -16 | | | |
| 120 | 7348 | 35 | | 3 | 35 | 10 | | | |

| | | | | | | | | | |
|---|---|---|---|---|---|---|---|---|---|
| | | | | | | | | | |
| Rocktype | | | Crow Mountain Sandstone | | | | | | |
| | | | ft | in | | | | | |
| Stratigraphic thickness | | | 21 | 6 | | | | | |
| Bedding orientation | | | N63E | 32N | | | | | |
| | | | | | | | | | |
| DATA | | | | | | | | | |
| **Scanline length** | **Leg** | **Orientation** | | **Trace length** | | **Terminations** | | **Movement** | **Comments** |
| Ft (decimal) | | Strike | Dip | Ft | In | Upper | Lower | | |
| 2 | 1 | N08E | 73S | 6 | 3 | U | U | | |
| 2.1 | 1 | N65E | 84W | 3 | 5 | A | A | | |
| 2.3 | 1 | N20W | 72S | 4 | 7 | U | U | | WIDTH 1" |
| 2.3 | 1 | N70E | 50E | 6 | 10 | T | A | | |
| 2.4 | 1 | N63E | 63E | 2 | 10 | A | U | | |
| 2.8 | 1 | N84E | 88W | 2 | 8 | H | A | | |
| 1 | 1 | N50W | 68S | 1 | 10 | U | U | | |
| 4.2 | 1 | N40E | 73S | 13 | 10 | U | U | | |
| 4.4 | 1 | N35E | 35E | 5 | 7 | A | A | | |
| 5.4 | 1 | N25E | 51E | 8 | 3 | U | A | | |
| 6.9 | 1 | N00S | 56E | 3 | 9 | T | A | | |
| 6.25 | 1 | N32E | 76E | 4 | 10 | A | A | | |
| 5.9 | 1 | N74E | 64S | 17 | 6 | U | U | REVERSE > 1 FT | WIDTH 1" |
| 8.2 | 1 | N00S | 70E | 5 | 7 | U | T | | |
| 8 | 1 | N29E | 74E | 2 | 7 | T | A | | |
| 8.6 | 1 | N42E | 76E | 6 | 9 | A | U | | |
| 8.3 | 1 | N02E | 39E | 14 | 2 | H | U | RIGHT LATERAL | WIDTH 1" |
| 8.9 | 1 | N19E | 45E | 6 | 6 | A | T | | |
| 10.2 | 1 | N59E | 53E | 9 | 1 | A | A | | |
| 10.5 | 1 | N66W | 70S | 2 | 4 | A | A | | |
| 11 | 1 | N46E | 60E | 20 | 6 | A | U | RIGHT LATERAL | |
| 11.05 | 1 | N68W | 66S | 6 | 0 | U | T | | |
| 12.8 | 1 | N15E | 42E | 6 | 0 | A | T | | |
| 14.8 | 1 | N36E | 56E | 17 | 0 | U | A | | |
| 16.5 | 2 | N12E | 70E | 6 | 2 | U | T | | |
| 17.1 | 2 | N70W | 64S | 6 | 7 | U | B | | |
| 17.1 | 2 | N15E | 59E | 11 | 0 | U | A | | |
| 18.3 | 2 | N70W | 71S | 5 | 1 | U | T | | |
| 20.6 | 2 | N69W | 63S | 4 | 9 | A | U | | |
| 21.3 | 2 | N42W | 71S | 4 | 4 | T | B | | |
| 22.6 | 2 | N85W | 62S | 4 | 6 | T | T | | |
| 22.3 | 2 | N12E | 58E | 2 | 0 | U | U | | |
| 23.4 | 2 | N52W | 82W | 4 | 10 | T | A | | |
| 24 | 2 | N48W | 70W | 13 | 1 | U | U | | |
| 25.9 | 2 | N58W | 77W | 4 | 0 | A | T | | |
| 27.2 | 3 | N52W | 70W | 5 | 4 | U | T | | |

| | | | | | | | | | |
|---|---|---|---|---|---|---|---|---|---|
| 27.85 | 3 | N57W | 78W | 4 | 10 | U | A | | |
| 28.3 | 3 | N69W | 66W | 12 | 3 | T | U | | |
| 29.15 | 3 | N85E | 83S | 1 | 7 | U | A | | |
| 29.4 | 3 | N60W | 75W | 6 | 7 | U | T | | |
| 30.35 | 3 | N73E | 86S | 8 | 1 | T | A | | |
| 30.4 | 3 | N80W | 46S | 2 | 6 | U | T | | |
| 29.9 | 3 | N59W | 52E | 1 | 0 | T | U | | |
| 31.4 | 3 | N85E | 50S | 9 | 2 | T | T | | |
| 31.1 | 3 | N60W | 62W | 3 | 3 | U | A | | |
| 31.5 | 3 | N50W | 77W | 23 | 1 | U | U | | |
| 32.6 | 3 | N60W | 72W | 1 | 11 | A | U | ? | FAULT |
| 32.8 | 3 | N38W | 78W | 2 | 2 | U | T | | |
| 33.6 | 3 | N74W | 78S | 1 | 11 | U | T | | |

### 6.2.3 SCANLINE 3

| | | | | | | | | | |
|---|---|---|---|---|---|---|---|---|---|
| Scanline Data | 070300 | | | | | | | | |
| Name | SCANLINE_3 | | | | | | | | |
| | | | | | | | | | |
| GPS points along the scan line | | | | | | | | | |
| Waypoint | Altitude | Scanline distance (ft) | | Leg | Orientation | | | | |
| 121 | 7342 | 2 | | | | | | | |
| 122 | 7348 | 21 | | 1 | 26 | -2 | | | |
| | | | | | | | | | |
| | | | | | | | | | |
| | | | | | | | | | |
| Rocktype | | | Red Peak Siltstone | | | | | | |
| | | | ft | in | | | | | |
| Stratigraphic thickness | | | | | | | | | |
| Bedding orientation | | | N26E | 32N | | | | | |
| | | | | | | | | | |
| DATA | | | | | | | | | |
| **Scanline length** | **Leg** | **Orientation** | | **Trace length** | | **Terminations** | | **Movement** | **Comments** |
| Ft (decimal) | | Strike | Dip | Ft | In | Upper | Lower | | |
| 1.9 | 1 | N45W | 71E | 1 | 11 | A | T | | |
| 2.6 | 1 | N07W | 43W | 6 | 0 | A | U | | |
| 3.1 | 1 | N77W | 67E | 11 | 0 | U | T | | |
| 3.25 | 1 | N83W | 31S | 3 | 10 | T | A | | |
| 4.2 | 1 | N47W | 90 | 4 | 4 | U | U | | |
| 5 | 1 | N80W | 78N | 2 | 3 | H | H | | |
| 5.1 | 1 | N58W | 23S | 6 | 6 | T | T | | |
| 6.65 | 1 | N39W | 75E | 4 | 5 | T | A | | |
| 7.4 | 1 | N81E | 75E | 2 | 2 | T | U | | |
| 7.3 | 1 | N82W | 28S | 6 | 2 | T | U | | |

| | | | | | | | | | |
|---|---|---|---|---|---|---|---|---|---|
| 7.6 | 1 | N65E | 81N | 3 | 0 | T | U | | |
| 8 | 1 | N70E | 76N | 1 | 9 | T | B | | |
| 9.7 | 1 | N05W | 24S | 5 | 10 | T | T | | |
| 10 | 1 | N88E | 60N | 1 | 11 | T | T | | |
| 9.7 | 1 | N56E | 82E | 2 | 5 | T | A | | |
| 11.15 | 1 | N78E | 88S | 6 | 2 | U | U | | |
| 10.5 | 1 | N75W | 81N | 3 | 4 | U | A | | |
| 12.3 | 1 | N68E | 78S | 3 | 8 | T | A | | |
| 13.1 | 1 | N67E | 70N | 3 | 0 | T | T | | |
| 12.9 | 1 | N65W | 25S | 7 | 9 | U | T | | |
| 15 | 1 | N55W | 25S | 1 | 7 | H | H | | |
| 15.37 | 1 | N41W | 31S | 5 | 5 | U | T | | |
| 16.25 | 1 | N55E | 81N | 1 | 5 | T | T | | |
| 17.02 | 1 | N25W | 25S | 3 | 8 | T | H | | |
| 17.35 | 1 | N66W | 29S | 1 | 3 | T | H | | |
| 17.5 | 1 | N61E | 88S | 3 | 10 | B | B | | |
| 18.25 | 1 | N69W | 28S | 7 | 3 | U | A | | |
| 18.8 | 1 | N51E | 88N | 4 | 9 | U | B | | |
| 19.7 | 1 | N55E | 84N | 2 | 8 | U | T | | |
| 18.4 | 1 | N71E | 40N | 8 | 8 | A | A | | |
| 20.9 | 1 | N41W | 19S | 3 | 11 | U | T | | |

### 6.2.4 SCANLINE 4

| | | | | | | | | | |
|---|---|---|---|---|---|---|---|---|---|
| Scanline Data | 070400 | | | | | | | | |
| Name | SCANLINE_4 | | | | | | | | |
| | | | | | | | | | |
| GPS points along the scan line | | | | | | | | | |
| Waypoint | Altitude | Scanline distance (ft) | | Leg | Orientation | | | | |
| 124 | 7295 | 2 | | | | | | | |
| 125 | 7303 | 35 | | 1 | 347 | -6 | | | |
| | | | | | | | | | |
| | | | | | | | | | |
| | | | | | | | | | |
| Rocktype | | | Crow Mountain | | | | | | |
| | | | ft | in | | | | | |
| Stratigraphic thickness | | | 14 | 4 | | | | | |
| Bedding orientation | | | N24W | 44S | | | | | |
| | | | | | | | | | |
| DATA | | | | | | | | | |
| **Scanline length** | **Leg** | **Orientation** | | **Trace length** | | **Terminations** | | **Movement** | **Comments** |
| Ft (decimal) | | Strike | Dip | Ft | In | Upper | Lower | | |
| 2.25 | 1 | N75E | 66W | 1 | 10 | T | T | | |

| | | | | | | | | | |
|---|---|---|---|---|---|---|---|---|---|
| 2.6 | 1 | N82E | 58W | 0 | 11 | T | T | | |
| 3.1 | 1 | N38E | 74W | 2 | 5 | T | A | | |
| 3.25 | 1 | N82E | 90E | 4 | 2 | U | T | | |
| 3.8 | 1 | N58E | 88E | 13 | 9 | U | U | | |
| 4.15 | 1 | N46W | 55S | 7 | 8 | A | A | | |
| 4.53 | 1 | N58E | 86S | 2 | 10 | U | T | | |
| 4.82 | 1 | N58E | 89N | 3 | 1 | U | U | | |
| 5 | 1 | N55E | 90E | 1 | 7 | T | T | | |
| 5.45 | 1 | N55E | 77S | 5 | 8 | U | U | | |
| 6.5 | 1 | N40E | 75S | 2 | 11 | T | T | | |
| 7.4 | 1 | N30E | 65E | 1 | 6 | T | B | | |
| 7.5 | 1 | N59E | 85S | 3 | 11 | B | U | | |
| 7.55 | 1 | N83E | 79N | 4 | 3 | H | T | | |
| 7.9 | 1 | N37E | 75E | 1 | 6 | A | U | | |
| 7.3 | 1 | N50E | 73E | 3 | 0 | T | B | | |
| 8.05 | 1 | N68E | 84S | 1 | 7 | T | T | | |
| 8.3 | 1 | N70E | 85S | 4 | 3 | U | T | | |
| 9.1 | 1 | N48E | 90E | 2 | 2 | A | T | | |
| 8.95 | 1 | N41E | 79N | 1 | 9 | AQ | A | | |
| 9.6 | 1 | N74E | 79S | 2 | 2 | A | T | | |
| 10.2 | 1 | N74E | 82S | 2 | 2 | B | U | | |
| 10.5 | 1 | N43W | 51S | 8 | 2 | A | A | | |
| 10.7 | 1 | N88W | 85S | 2 | 1 | B | U | | |
| 10.9 | 1 | N71E | 87S | 1 | 11 | A | U | | |
| 11.85 | 1 | N45E | 79S | 3 | 2 | H | U | | |
| 12.4 | 1 | N54E | 70S | 5 | 3 | U | U | | |
| 13.4 | 1 | N61E | 82S | 2 | 8 | T | U | | |
| 13.7 | 1 | N76E | 85S | 4 | 6 | U | U | | |
| 14.2 | 1 | N58E | 84S | 1 | 6 | A | U | | |
| 15.6 | 1 | N55E | 88S | 12 | 11 | T | U | | |
| 15.15 | 1 | N86W | 73S | 4 | 6 | A | T | | |
| 15.5 | 1 | N62E | 87S | 1 | 2 | A | U | | |
| 16 | 1 | N60E | 90E | 4 | 11 | U | U | | |
| 16.6 | 1 | N58E | 82S | 2 | 3 | U | U | | |
| 17.2 | 1 | N60E | 87S | 3 | 6 | A | T | | |
| 17.3 | 1 | N64E | 83S | 13 | 5 | U | U | | |
| 18.9 | 1 | N64E | 79S | 4 | 4 | U | A | | |
| 19.7 | 1 | N67E | 82S | 1 | 6 | T | U | | |
| 19.85 | 1 | N77E | 86S | 14 | 3 | U | U | | |
| 21 | 1 | N65E | 87S | 6 | 8 | H | A | | |
| 21.25 | 1 | N59E | 76S | 11 | 1 | H | A | | |
| 21.85 | 1 | N52E | 87S | 7 | 4 | U | U | | |
| 22.25 | 1 | N84E | 82S | 4 | 9 | A | U | | |
| 23.1 | 1 | N70E | 45S | 2 | 0 | B | T | | |
| 23.15 | 1 | N80E | 63S | 0 | 9 | U | U | | |
| 23.4 | 1 | N64E | 68S | 0 | 9 | T | U | | |
| 24.9 | 1 | N52E | 61S | 3 | 1 | U | T | | |

| | | | | | | | | | |
|---|---|---|---|---|---|---|---|---|---|
| 25.5 | 1 | N66E | 72S | 3 | 2 | T | T | | |
| 25.8 | 1 | N58E | 80S | 3 | 9 | T | U | | |
| 26.6 | 1 | N31E | 66S | 2 | 7 | A | U | | |
| 25.9 | 1 | N81E | 75N | 1 | 11 | A | U | | |
| 25.15 | 1 | N57E | 72S | 3 | 8 | T | T | | |
| 27.6 | 1 | N24E | 68S | 3 | 10 | U | U | | |
| 28.9 | 1 | N23E | 62S | 14 | 0 | A | U | ? | FAULT WITH PARALLEL FRACTURES |
| 29 | 1 | N55E | 85S | 4 | 2 | U | U | | |
| 29.6 | 1 | N64E | 90W | 1 | 8 | A | T | | |
| 30 | 1 | N50E | 76S | 2 | 3 | A | T | | |
| 30.9 | 1 | N32E | 78S | 3 | 0 | U | T | | |
| 31.1 | 1 | N66E | 87N | 5 | 0 | U | U | | |
| 31.95 | 1 | N25E | 90W | 1 | 8 | A | A | | |
| 32 | 1 | N52E | 88S | 5 | 2 | U | U | | |
| 32.4 | 1 | N44E | 89N | 13 | 7 | U | U | | |
| 33.35 | 1 | N53E | 84S | 1 | 10 | H | B | | |
| 33.4 | 1 | N72E | 90E | 2 | 6 | T | T | | |
| 33.7 | 1 | N69E | 79S | 2 | 9 | U | T | | |
| 34 | 1 | N63E | 89S | 3 | 5 | U | U | | |
| 34.3 | 1 | N65E | 77S | 4 | 4 | U | A | | |
| 35.35 | 1 | N49E | 88S | 3 | 2 | U | U | | |

## 6.2.5 SCANLINE 5

| | | | | | | | | | |
|---|---|---|---|---|---|---|---|---|---|
| Scanline Data | 070500 | | | | | | | | |
| Name | SCANLINE_5 | | | | | | | | |
| | | | | | | | | | |
| GPS points along the scan line | | | | | | | | | |
| Waypoint | Altitude | Scanline distance (ft) | | Leg | Orientation | | | | |
| 126 | 7335 | 1 | | | | | | | |
| 127 | 7338 | 33 | | 1 | 143 | -10 | | | |
| | | | | | | | | | |
| | | | | | | | | | |
| | | | | | | | | | |
| Rocktype | | | Crow Mountain | | | | | | |
| | | | ft | in | | | | | |
| Stratigraphic thickness | | | >12 | | | | | | |
| Bedding orientation | | | N45W | 33N | | | | | |
| | | | | | | | | | |
| DATA | | | | | | | | | |
| **Scanline length** | **Leg** | **Orientation** | | **Trace length** | | **Terminations** | | **Movement** | **Comments** |
| Ft (decimal) | | Strike | Dip | Ft | In | Upper | Lower | | |

| | | | | | | | | | |
|---|---|---|---|---|---|---|---|---|---|
| 4.4 | 1 | N68W | 52S | 20 | 0 | U | B | | |
| 9.7 | 1 | N74W | 52S | 5 | 6 | T | U | | |
| 16.7 | 1 | N88E | 90S | 7 | 6 | H | B | | |
| 17.02 | 1 | N79E | 80S | 13 | 0 | U | H | | |
| 16.9 | 1 | N60W | 57S | 3 | 5 | B | H | | |
| 17 | 1 | N47W | 59S | 8 | 7 | T | U | | FAULT |
| 24.2 | 1 | N54E | 79W | 3 | 0 | T | T | | |
| 25.8 | 1 | N84W | 58S | 6 | 5 | T | T | | |
| 27.4 | 1 | N21E | 82W | 10 | 0 | U | T | | |
| 28.5 | 1 | N80E | 78S | 1 | 6 | T | T | | |
| 25 | 1 | N58W | 55S | 1 | 6 | A | B | | |
| 24.3 | 1 | N48W | 56S | 7 | 0 | T | B | | |
| 29.4 | 1 | N70W | 48S | 6 | 5 | T | B | | |
| 29.9 | 1 | N45E | 80N | 7 | 0 | T | B | | |
| 29.7 | 1 | N68W | 78S | 2 | 2 | T | U | | |
| 32.3 | 1 | N89E | 73N | 5 | 4 | T | T | | |
| 34.15 | 1 | N60W | 52S | 6 | 5 | U | U | | |

### 6.2.6 SCANLINE 6

| | | | | | | | | | |
|---|---|---|---|---|---|---|---|---|---|
| Scanline Data | 070500 | | | | | | | | |
| Name | SCANLINE_6 | | | | | | | | |
| | | | | | | | | | |
| GPS points along the scan line | | | | | | | | | |
| Waypoint | Altitude | Scanline distance (ft) | | Leg | Orientation | | | | |
| 129 | 7314 | 0 | | | | | | | |
| 131 | 7332 | 31 | | 1 | 138 | -6 | | | |
| | | | | | | | | | |
| | | | | | | | | | |
| | | | | | | | | | |
| Rocktype | | | Crow Mountain | | | | | | |
| | | | ft | in | | | | | |
| Stratigraphic thickness | | | | | | | | | |
| Bedding orientation | | | N46W | 30N | | | | | |
| | | | | | | | | | |
| DATA | | | | | | | | | |
| **Scanline length** | **Leg** | **Orientation** | | **Trace length** | | **Terminations** | | **Movement** | **Comments** |
| Ft (decimal) | | Strike | Dip | Ft | In | Upper | Lower | | |
| 0.1 | 1 | N81E | 88S | 18 | 0 | A | T | | |
| 0.42 | 1 | N67E | 87S | 5 | 1 | B | U | | |
| 0.58 | 1 | N64E | 83S | 1 | 9 | B | A | | |
| 0.77 | 1 | N67E | 88N | 4 | 1 | T | H | | |

| | | | | | | | | | |
|---|---|---|---|---|---|---|---|---|---|
| 1.15 | 1 | N85E | 74N | 1 | 2 | B | U | | |
| 1.45 | 1 | N88W | 69N | 2 | 10 | T | H | | |
| 1.7 | 1 | N86E | 88N | 2 | 9 | B | A | | |
| 1.81 | 1 | N81E | 85S | 0 | 8 | A | T | | |
| 2.02 | 1 | N58E | 85S | 1 | 3 | A | A | | |
| 2.4 | 1 | N80E | 76N | 1 | 1 | U | A | | |
| 2.95 | 1 | N53E | 58S | 4 | 5 | B | U | | |
| 2.9 | 1 | N76E | 89S | 2 | 2 | T | A | | |
| 2.1 | 1 | N74E | 80N | 2 | 0 | T | B | | |
| 3.4 | 1 | N80E | 79N | 1 | 2 | T | T | | |
| 3.85 | 1 | N42E | 56S | 1 | 9 | A | U | | |
| 4.4 | 1 | N73E | 87S | 1 | 2 | T | A | | |
| 4.05 | 1 | N74W | 88S | 0 | 11 | T | B | | |
| 4.5 | 1 | N56E | 83S | 5 | 3 | B | A | | |
| 4.6 | 1 | N65E | 77N | 28 | 0 | U | U | | |
| 4.75 | 1 | N48E | 80S | 1 | 2 | A | A | | |
| 4.88 | 1 | N59E | 75S | 1 | 0 | H | B | | |
| 5.45 | 1 | N50E | 85S | 1 | 10 | B | T | | |
| 5.5 | 1 | N50E | 82N | 7 | 9 | A | U | | |
| 6.25 | 1 | N74E | 84S | 2 | 6 | U | U | | |
| 6.35 | 1 | N23E | 73E | 1 | 10 | T | A | | |
| 6.6 | 1 | N44E | 78S | 2 | 11 | A | H | | |
| 6.85 | 1 | N90E | 90S | 3 | 3 | T | U | | |
| 6.9 | 1 | N75E | 82N | 1 | 10 | H | A | | |
| 8 | 1 | N50E | 78S | 8 | 5 | A | B | | |
| 8.15 | 1 | N40E | 70E | 1 | 10 | A | T | | |
| 7.9 | 1 | N80E | 80N | 18 | 0 | U | A | | |
| 9.4 | 1 | N66E | 84N | 3 | 2 | B | B | | |
| 8.5 | 1 | N45E | 85N | 1 | 2 | B | A | | |
| 9.8 | 1 | N79W | 81N | 1 | 10 | B | U | | |
| 11 | 1 | N72E | 79N | 3 | 8 | A | U | | |
| 11.05 | 1 | N89W | 82N | 0 | 9 | H | H | | |
| 11.2 | 1 | N88W | 84N | 0 | 10 | T | T | | |
| 11.25 | 1 | N85W | 88N | 4 | 8 | H | A | | |
| 11.4 | 1 | N52E | 72S | 3 | 0 | A | U | | |
| 11.75 | 1 | N34E | 90S | 1 | 9 | A | U | | |
| 11.2 | 1 | N90E | 82S | 3 | 5 | T | U | | |
| 12.05 | 1 | N90E | 82S | 2 | 10 | H | U | | |
| 12.25 | 1 | N85W | 80S | 1 | 5 | A | H | | |
| 12.55 | 1 | N61E | 74S | 10 | 6 | A | U | | |
| 13.1 | 1 | N48E | 84S | 1 | 10 | B | A | | |
| 13 | 1 | N69E | 76N | 2 | 7 | T | T | | |
| 13.3 | 1 | N46E | 79S | 1 | 7 | T | A | | |
| 13.2 | 1 | N72E | 90S | 3 | 1 | B | U | | |
| 13.55 | 1 | N64E | 89S | 3 | 3 | H | U | | |
| 13.6 | 1 | N65E | 58S | 2 | 5 | A | T | | |
| 13.7 | 1 | N76E | 78S | 12 | 3 | A | U | | |

| | | | | | | | | | |
|---|---|---|---|---|---|---|---|---|---|
| 13.9 | 1 | N74E | 65S | 12 | 1 | A | T | | |
| 13.8 | 1 | N84W | 80N | 2 | 2 | T | A | | |
| 14.4 | 1 | N45E | 80S | 1 | 5 | A | T | | |
| 14.4 | 1 | N88E | 86N | 6 | 5 | T | U | | |
| 14.9 | 1 | N29E | 79E | 0 | 0 | A | A | | |
| 14.9 | 1 | N76E | 68N | 2 | 9 | B | A | | |
| 15.6 | 1 | N68E | 82S | 3 | 4 | T | A | | many B´s may and as T´s against bedding |
| 16 | 1 | N78E | 80N | 2 | 2 | T | T | | |
| 16.4 | 1 | N88W | 78S | 1 | 1 | B | B | | |
| 16.85 | 1 | N49E | 85N | 3 | 6 | T | A | | |
| 17.1 | 1 | N49E | 82S | 4 | 9 | T | U | | |
| 17.2 | 1 | N86E | 78N | 1 | 3 | B | A | | |
| 17.9 | 1 | N81E | 78N | 4 | 9 | B | A | | |
| 19 | 1 | N73E | 87N | 4 | 5 | B | U | | |
| 19.6 | 1 | N46E | 84S | 4 | 1 | A | A | | |
| 19.9 | 1 | N60E | 87S | 2 | 5 | T | A | | |
| 20.3 | 1 | N44E | 85S | 3 | 4 | T | A | | |
| 20.55 | 1 | N42E | 86N | 0 | 11 | T | T | | |
| 21 | 1 | N74E | 90S | 1 | 2 | A | A | | |
| 21.5 | 1 | N34E | 80S | 14 | 11 | U | A | | |
| 21.55 | 1 | N46E | 88N | 1 | 3 | T | B | | |
| 21.65 | 1 | N57E | 83N | 3 | 10 | T | T | | |
| 22.3 | 1 | N34E | 85N | 3 | 10 | A | T' | | |
| 22.8 | 1 | N53E | 44S | 3 | 1 | T | A | | |
| 23.5 | 1 | N46E | 88S | 5 | 6 | T | T | | GROUP |
| 24.1 | 1 | N52E | 75S | 5 | 0 | T | A | | |
| 24.1 | 1 | N88E | 84S | 3 | 8 | T | T | | |
| 24.55 | 1 | N48E | 66S | 1 | 7 | A | A | | |
| 24.35 | 1 | N42E | 75S | 1 | 3 | T | B | | |
| 24.8 | 1 | N80E | 82S | 4 | 6 | T | U | | |
| 25.1 | 1 | N76E | 88S | 6 | 1 | T | A | | |
| 25.7 | 1 | N75E | 82S | 2 | 11 | B | U | | |
| 24.7 | 1 | N55W | 76S | 3 | 2 | B | U | | |
| 26.8 | 1 | N38E | 84S | 3 | 4 | B | U | | |
| 30.8 | 1 | N48E | 80S | 4 | 1 | T | T | | |
| 29 | 1 | N84W | 90S | 1 | 4 | B | B | | |

### 6.2.7 SCANLINE 7

| | | | | | | | | | |
|---|---|---|---|---|---|---|---|---|---|
| Scanline Data | 070500 | | | | | | | | |
| Name | SCANLINE_7 | | | | | | | | |

| | | | | | | | | | |
|---|---|---|---|---|---|---|---|---|---|
| | | | | | | | | | |
| GPS points along the scan line | | | | | | | | | |
| Waypoint | Altitude | Scanline distance (ft) | | Leg | Orientation | | | | |
| 132 | 7306 | 0 | | | | | | | |
| 133 | 7303 | 54 | | 1 | 195 | -4 | | | |
| | | | | | | | | | |
| | | | | | | | | | |
| | | | | | | | | | |
| Rocktype | | | Crow Mountain | | | | | | |
| | | | ft | in | | | | | |
| Stratigraphic thickness | | | 10 | | | | | | |
| Bedding orientation | | | N20E | 25E | | | | | |
| | | | | | | | | | |
| DATA | | | | | | | | | |
| **Scanline length** | **Leg** | **Orientation** | | **Trace length** | | **Terminations** | | **Movement** | **Comments** |
| Ft (decimal) | | Strike | Dip | Ft | In | Upper | Lower | | |
| 1.4 | 1 | N14E | 77W | 3 | 1 | T | T | | |
| 1.6 | 1 | N35E | 75W | 5 | 0 | T | T | | |
| 1.3 | 1 | N74E | 75N | 3 | 3 | T | A | | |
| 1.6 | 1 | N74E | 75N | 5 | 2 | T | B | | |
| 2.1 | 1 | N70E | 80N | 5 | 10 | T | B | | |
| 3 | 1 | N56W | 70S | 1 | 2 | T | T | | |
| 4.3 | 1 | N64E | 82N | 35 | 0 | T | U | | |
| 4.35 | 1 | N68E | 68N | 1 | 0 | A | A | | |
| 4.7 | 1 | N75W | 85N | 2 | 6 | A | B | | |
| 5.27 | 1 | N75E | 86N | 1 | 6 | T | B | | |
| 6 | 1 | N74E | 76N | 4 | 8 | B | T | | |
| 7.1 | 1 | N66E | 85N | 1 | 4 | H | H | | |
| 7.4 | 1 | N90E | 89N | 26 | 0 | A | B | | |
| 13.9 | 1 | N90E | 70S | 50 | 0 | U | B | | |
| 9.2 | 1 | N85W | 72N | 5 | 2 | H | T | | |
| 8.5 | 1 | N69W | 72N | 1 | 10 | A | T | | |
| 9.7 | 1 | N84E | 74N | 0 | 6 | T | T | | |
| 10 | 1 | N89E | 85N | 0 | 6 | T | T | | |
| 10.3 | 1 | N85E | 90S | 2 | 4 | H | B | | |
| 10.7 | 1 | N82E | 78N | 7 | 10 | T | T | | |
| 11.7 | 1 | N70E | 75N | 3 | 2 | H | B | | |
| 14.7 | 1 | N15W | 85W | 3 | 5 | U | T | | |
| 17.7 | 1 | N20W | 20W | 0 | 11 | A | U | | |
| 18.6 | 1 | N72W | 78S | 6 | 6 | T | T | | |
| 19.8 | 1 | N70W | 84N | 0 | 11 | T | T | | |
| 19 | 1 | N44W | 68N | 2 | 11 | T | B | | |
| 20.4 | 1 | N76W | 80N | 6 | 7 | T | T | | |
| 21.6 | 1 | N68W | 90S | 0 | 10 | B | T | | |
| 22.5 | 1 | N72W | 80N | 5 | 8 | A | T | | |
| 23.3 | 1 | N70W | 70N | 9 | 10 | A | T | | |

| | | | | | | | | | |
|---|---|---|---|---|---|---|---|---|---|
| 23.55 | 1 | N75W | 75S | 5 | 10 | T | B | | |
| 25.7 | 1 | N78W | 65S | 8 | 0 | T | A | | |
| 26.5 | 1 | N60E | 84S | 1 | 11 | A | A | | |
| 26.5 | 1 | N78W | 73N | 3 | 6 | T | H | | |
| 26.35 | 1 | N33W | 58W | 0 | 12 | T | T | | |
| 27.5 | 1 | N80E | 90S | 1 | 3 | T | T | | |
| 27.7 | 1 | N76W | 84N | 1 | 3 | T | T | | |
| 29.45 | 1 | N86W | 65S | 9 | 7 | T | T | | |
| 32.1 | 1 | N62W | 67S | 3 | 5 | T | T | | |
| 32.5 | 1 | N58W | 74S | 3 | 2 | T | A | | |
| 32.3 | 1 | N46W | 62S | 3 | 7 | H | A | | |
| 34 | 1 | N64W | 64S | 6 | 5 | T | T | | |
| 36.2 | 1 | N75E | 80N | 3 | 4 | T | T | | |
| 36.9 | 1 | N52W | 70S | 2 | 7 | T | T | | |
| 37.4 | 1 | N30W | 80S | 4 | 3 | T | B | | |
| 37.9 | 1 | N56W | 72S | 2 | 8 | B | B | | |
| 39.3 | 1 | N57W | 74S | 6 | 8 | U | B | | |
| 40.1 | 1 | N68W | 85N | 4 | 5 | B | A | | |
| 40.5 | 1 | N46W | 82S | 2 | 4 | T | B | | |
| 41.8 | 1 | N89E | 82N | 2 | 1 | T | T | | |
| 41.3 | 1 | N8E | 57W | 1 | 1 | U | T | | |
| 42.5 | 1 | N62W | 80S | 8 | 2 | T | U | | |
| 43.1 | 1 | N57W | 84S | 3 | 10 | U | B | | |
| 42.6 | 1 | N68W | 82S | 0 | 0 | T | T | | |
| 43.6 | 1 | N65W | 77S | 2 | 4 | B | B | | |
| 44.2 | 1 | N56W | 70S | 3 | 8 | U | B | | |
| 44.8 | 1 | N44W | 69S | 1 | 7 | T | B | | |
| 45.5 | 1 | N49W | 66S | 6 | 0 | T | T | | |
| 46.7 | 1 | N75E | 85N | 2 | 3 | B | B | | |
| 47 | 1 | N52W | 76S | 1 | 3 | T | B | | |
| 47.4 | 1 | N46W | 77S | 6 | 5 | U | T | | |
| 48.3 | 1 | N55W | 80S | 4 | 1 | U | B | | |
| 48.8 | 1 | N46W | 83S | 50 | 0 | U | U | | |
| 50.45 | 1 | N74W | 58S | 50 | 0 | U | T | | |
| 49.3 | 1 | N64E | 34S | 0 | 12 | T | A | | |
| 51.4 | 1 | N62W | 80N | 3 | 5 | U | A | | |
| 53.1 | 1 | N55W | 82S | 0 | 12 | T | T | | |
| 53.85 | 1 | N55W | 83S | 2 | 11 | T | T | | |

### 6.2.8 SCANLINE 8

| | | | | | | | | | |
|---|---|---|---|---|---|---|---|---|---|
| Scanline Data | 070600 | | | | | | | | |
| Name | SCANLINE_8 | | | | | | | | |
| | | | | | | | | | |

| | | | | | | | | | |
|---|---|---|---|---|---|---|---|---|---|
| GPS points along the scan line | | | | | | | | | |
| Waypoint | Altitude | Scanline distance (ft) | | Leg | Orientation | | | | |
| 134 | 7218 | 0 | | | | | | | |
| 135 | 7226 | 21 | | 1 | 180 | -5 | | | |
| 136 | 7225 | 36 | | 2 | 165 | 2 | | | |
| | | | | | | | | | |
| | | | | | | | | | |
| Rocktype | | | Red Peak | | | | | | |
| | | | ft | in | | | | | |
| Stratigraphic thickness | | | | | | | | | |
| Bedding orientation | | | N6W | 11E | | | | | |
| | | | | | | | | | |
| DATA | | | | | | | | | |
| **Scanline length** | **Leg** | **Orientation** | | **Trace length** | | **Terminations** | | **Movement** | **Comments** |
| Ft (decimal) | | Strike | Dip | Ft | In | Upper | Lower | | |
| 0.5 | 1 | N85W | 78S | 2 | 7 | T | U | | |
| 0.8 | 1 | N86W | 80S | 0 | 9 | T | A | | |
| 0.9 | 1 | N84W | 82S | 0 | 7 | B | B | | |
| 1.5 | 1 | N89E | 85S | 1 | 8 | B | B | | |
| 1.1 | 1 | N58W | 90S | 3 | 8 | A | U | | |
| 2.5 | 1 | N80E | 90S | 10 | 0 | U | U | | $CaCO_3$ filled |
| 2.7 | 1 | N71W | 74N | 2 | 0 | B | A | | |
| 3.1 | 1 | N76W | 86N | 4 | 0 | A | U | | |
| 3.4 | 1 | N85E | 85N | 1 | 5 | B | U | | |
| 3.8 | 1 | N70E | 90S | 5 | 4 | A | U | | |
| 3.2 | 1 | N76W | 74N | 5 | 7 | A | U | | |
| 4.4 | 1 | N90W | 66S | 1 | 3 | A | B | | |
| 4.9 | 1 | N89W | 67N | 7 | 10 | U | U | | |
| 5.2 | 1 | N79W | 88N | 2 | 0 | A | U | | |
| 5.5 | 1 | N65E | 66N | 1 | 3 | H | T | | |
| 6.6 | 1 | N72W | 68S | 1 | 4 | T | B | | |
| 6.4 | 1 | N24W | 81S | 4 | 2 | T | T | | |
| 9.2 | 1 | N84W | 84N | 4 | 6 | T | A | | |
| 9.6 | 1 | N85E | 85N | 2 | 10 | H | U | | |
| 9.3 | 1 | N00E | 30E | 2 | 1 | T | U | | |
| 10.9 | 1 | N64W | 85N | 5 | 0 | A | T | | |
| 11.5 | 1 | N88E | 78S | 2 | 6 | A | A | | |
| 11.8 | 1 | N85E | 86S | 9 | 0 | U | U | | |
| 13.8 | 1 | N69W | 38S | 4 | 2 | T | T | | |
| 14.9 | 1 | N88E | 80S | 10 | 0 | U | U | | |
| 14.8 | 1 | N64W | 33N | 4 | 7 | T | T | | |
| 16.1 | 1 | N56W | 80N | 1 | 4 | T | B | | |
| 16.4 | 1 | N58W | 90N | 1 | 10 | H | T | | |
| 16.6 | 1 | N42W | 90N | 4 | 2 | B | A | | |
| 16.5 | 1 | N64W | 90S | 4 | 5 | A | A | | |
| 17 | 1 | N10W | 75W | 2 | 0 | T | T | | |

| | | | | | | | | | |
|---|---|---|---|---|---|---|---|---|---|
| 19.6 | 1 | N78W | 82N | 6 | 6 | T | U | | |
| 20.5 | 1 | N40W | 85S | 3 | 0 | T | A | | |
| 22.3 | 2 | N68W | 90N | 8 | 1 | T | U | | |
| 24.1 | 2 | N48E | 80N | 7 | 6 | T | U | | |
| 28.6 | 2 | N16E | 55W | 4 | 11 | H | U | | |
| 26.2 | 2 | N88W | 85S | 7 | 7 | U | U | | |
| 24.2 | 2 | N45W | 62S | 7 | 7 | A | U | | |
| 27.5 | 2 | N76E | 86S | 5 | 0 | T | U | | |
| 27.2 | 2 | N88E | 63N | 3 | 5 | T | A | | |
| 30.2 | 2 | N88E | 62S | 3 | 10 | T | T | | |
| 30.5 | 2 | N66W | 75S | 3 | 8 | H | H | | |
| 31.6 | 2 | N62E | 82N | 5 | 4 | H | U | | |
| 32.1 | 2 | N85W | 85S | 5 | 3 | T | U | | |
| 33.4 | 2 | N86E | 60S | 3 | 0 | T | A | | |
| 33.7 | 2 | N90W | 90S | 4 | 9 | U | A | | |
| 32.6 | 2 | N69W | 50N | 1 | 2 | U | T | | |
| 34.4 | 2 | N89E | 85S | 7 | 8 | U | U | | |
| 34.9 | 2 | N82W | 90N | 7 | 4 | U | U | | |
| 35.1 | 2 | N70W | 82S | 3 | 8 | B | A | | |
| 38.3 | 2 | N01E | 75W | 5 | 2 | U | T | | $CaCO_3$ not dominant |
| 40.1 | 2 | N01W | 74W | 3 | 2 | T | T | | $CaCO_3$ not dominant |
| 43.5 | 2 | N56E | 52S | 7 | 0 | T | U | | $CaCO_3$ not dominant |
| 43.2 | 2 | N86W | 69N | 1 | 10 | U | U | | $CaCO_3$ not dominant |
| 37 | 2 | N25E | 76W | 5 | 1 | U | T | | $CaCO_3$ not dominant |
| 41.5 | 2 | N60E | 82N | 1 | 2 | U | U | | $CaCO_3$ not dominant |

### 6.2.9 SCANLINE 9

| | | | | | | | | | |
|---|---|---|---|---|---|---|---|---|---|
| Scanline Data | 070600 | | | | | | | | |
| Name | SCANLINE_9 | | | | | | | | |
| | | | | | | | | | |
| GPS points along the scan line | | | | | | | | | |
| Waypoint | Altitude | Scanline distance (ft) | | Leg | Orientation | | | | |
| 139 | 7058 | 0 | | | | | | | |
| 140 | 7012 | 40 | | 1 | 192 | 0 | | | |
| | | | | | | | | | |
| | | | | | | | | | |
| | | | | | | | | | |
| Rocktype | | | Red Peak | | | | | | |
| | | | ft | in | | | | | |

| | | | | | | | | | |
|---|---|---|---|---|---|---|---|---|---|
| Stratigraphic thickness | | | 27 | 0 | | | | | |
| Bedding orientation | | | N14E | 24E | | | | | |
| | | | | | | | | | |
| DATA | | | | | | | | | |
| **Scanline length** | **Leg** | **Orientation** | | **Trace length** | | **Terminations** | | **Movement** | **Comments** |
| Ft (decimal) | | Strike | Dip | Ft | In | Upper | Lower | | |
| 2.3 | 1 | N64W | 74N | 11 | 0 | T | U | | Calcite filled |
| 2.5 | 1 | N78W | 78S | 1 | 3 | B | T | | Calcite filled |
| 3.1 | 1 | N86W | 86S | 1 | 7 | B | T | | Calcite filled |
| 5.1 | 1 | N87W | 87S | 1 | 10 | T | T | | Calcite filled |
| 5.25 | 1 | N41W | 49N | 4 | 8 | A | T | | Calcite filled |
| 7 | 1 | N56W | 83N | 3 | 11 | T | U | | Calcite filled |
| 7.15 | 1 | N62W | 72N | 4 | 3 | T | U | | Calcite filled |
| 8.9 | 1 | N65W | 77N | 17 | 0 | U | U | | Calcite filled |
| 11 | 1 | N45W | 61N | 5 | 3 | T | U | | Calcite filled |
| 11.3 | 1 | N37W | 65N | 3 | 6 | T | A | | Calcite filled |
| 13.3 | 1 | N69W | 81N | 17 | 0 | A | U | | Calcite filled |
| 16.7 | 1 | N70W | 84N | 14 | 4 | T | U | | Calcite filled |
| 18 | 1 | N64W | 65N | 4 | 4 | T | U | | Calcite filled |
| 23.2 | 1 | N67W | 87N | 14 | 0 | T | U | | Calcite filled |
| 28.6 | 1 | N72W | 86N | 5 | 9 | H | U | | Calcite filled |
| 28.7 | 1 | N75W | 86N | 10 | 8 | A | U | | Calcite filled |
| 24.7 | 1 | N72W | 90N | 1 | 1 | B | T | | |
| 26.3 | 1 | N10E | 47E | 5 | 10 | A | T | | |
| 29.1 | 1 | N10W | 47E | 3 | 8 | A | T | | |
| 33 | 1 | N76W | 90S | 0 | 10 | T | T | | |
| 33.5 | 1 | N61W | 79N | 11 | 0 | U | H | | |
| 33.6 | 1 | N84W | 78N | 7 | 10 | H | U | | |
| 35.6 | 1 | N75W | 73N | 9 | 10 | A | U | | |
| 37.9 | 1 | N25E | 75W | 4 | 6 | T | T | | |
| 37.3 | 1 | N10W | 29E | 4 | 5 | T | A | | |
| 39.2 | 1 | N19W | 30E | 5 | 2 | T | T | | |
| 40.1 | 1 | N59W | 65N | 13 | 0 | T | U | | |
| 41.3 | 1 | N56W | 71N | 13 | 0 | B | U | | |
| 41.9 | 1 | N40W | 38N | 8 | 11 | U | A | | |
| 43.2 | 1 | N08E | 75W | 4 | 4 | U | U | | |
| 45 | 1 | N20W | 52N | 4 | 7 | U | H | | |
| 48.5 | 1 | N64W | 47N | 10 | 10 | A | U | | |
| 49.6 | 1 | N88W | 63S | 3 | 1 | T | T | | |
| 51.9 | 1 | N78W | 68N | 6 | 0 | H | T | | |
| 52.1 | 1 | N40W | 79N | 1 | 5 | H | T | | |
| 53.3 | 1 | N82W | 67N | 3 | 9 | T | A | | |
| 54 | 1 | N80E | 73N | 0 | 12 | T | A | | |
| 54.7 | 1 | N82W | 88N | 35 | 0 | U | U | | |
| 55.4 | 1 | N18W | 85E | 3 | 10 | T | U | | |
| 56.2 | 1 | N76W | 85N | 4 | 5 | T | U | | |

| | | | | | | | | | |
|---|---|---|---|---|---|---|---|---|---|
| 56.3 | 1 | N72W | 87N | 1 | 6 | T | H | | |
| 57.4 | 1 | N62E | 88S | 13 | 0 | U | U | | |
| 58.25 | 1 | N57W | 70N | 3 | 4 | H | A | | |

### 6.2.10 SCANLINE 10

| | | | | | | | | | |
|---|---|---|---|---|---|---|---|---|---|
| Scanline Data | 070600 | | | | | | | | |
| Name | SCANLINE_10 | | | | | | | | |
| | | | | | | | | | |
| GPS points along the scan line | | | | | | | | | |
| Waypoint | Altitude | Scanline distance (ft) | | Leg | Orientation | | | | |
| 137 | 7150 | 0 | | | | | | | |
| 138 | 1760 | 40 | | 1 | 191 | 6 | | | |
| | | | | | | | | | |
| | | | | | | | | | |
| | | | | | | | | | |
| Rocktype | | | Red Peak | | | | | | |
| | | | ft | in | | | | | |
| Stratigraphic thickness | | | | | | | | | |
| Bedding orientation | | | | 15E | | | | | |
| | | | | | | | | | |
| DATA | | | | | | | | | |
| **Scanline length** | **Leg** | **Orientation** | | **Trace length** | | **Terminations** | | **Movement** | **Comments** |
| Ft (decimal) | | Strike | Dip | Ft | In | Upper | Lower | | |
| 1.3 | 1 | N62W | 84S | 2 | 7 | T | A | | |
| 1.4 | 1 | N64W | 87N | 6 | 0 | U | U | | |
| 3.2 | 1 | N41W | 78S | 3 | 0 | U | T | | |
| 4.4 | 1 | N62E | 69N | 3 | 0 | T | U | | |
| 4.7 | 1 | N39W | 80N | 2 | 10 | T | A | | |
| 6 | 1 | N70E | 73N | 2 | 7 | U | T | | |
| 7.5 | 1 | N50E | 70N | 1 | 0 | T | T | | |
| 8.9 | 1 | N63E | 70N | 6 | 0 | U | U | | |
| 7.8 | 1 | N32W | 80N | 2 | 3 | T | U | | |
| 10.7 | 1 | N48E | 85E | 4 | 8 | U | U | N25W 89W | |
| 9.8 | 1 | N57E | 57W | 2 | 10 | U | T | | |
| 11.6 | 1 | N72E | 70W | 1 | 8 | T | T | | |
| 12.3 | 1 | N72E | 70W | 0 | 8 | T | T | | |
| 13.3 | 1 | N62E | 75N | 2 | 0 | T | T | | |
| 14 | 1 | N43E | 87W | 1 | 8 | T | A | | |
| 13.7 | 1 | N84E | 64N | 7 | 5 | U | U | | |
| 12 | 1 | N30W | 90N | 3 | 5 | T | T | | |
| 16 | 1 | N75E | 67N | 3 | 4 | T | U | | |

| | | | | | | | | | |
|---|---|---|---|---|---|---|---|---|---|
| 17.1 | 1 | N69E | 66N | 1 | 1 | T | T | | |
| 16.6 | 1 | N26W | 19E | 2 | 10 | T | A | | |
| 18 | 1 | N82E | 55N | 1 | 3 | T | T | | |
| 18.2 | 1 | N65W | 65N | 0 | 11 | T | B | | |
| 18.8 | 1 | N76W | 55N | 1 | 10 | T | B | | |
| 18.9 | 1 | N80W | 76N | 8 | 2 | U | U | | |
| 20.1 | 1 | N66E | 74N | 1 | 2 | T | T | | |
| 20.1 | 1 | N78E | 82N | 0 | 7 | T | B | | |
| 20.8 | 1 | N40W | 90S | 2 | 0 | T | T | | |
| 21.8 | 1 | N41E | 69W | 2 | 5 | A | T | | |
| 23.6 | 1 | N49W | 75W | 2 | 9 | U | U | | |
| 24.8 | 1 | N61E | 73N | 4 | 10 | U | U | | |
| 24.4 | 1 | N82E | 71N | 2 | 11 | T | T | | |
| 26.5 | 1 | N80E | 67N | 4 | 3 | U | U | | |
| 25.7 | 1 | N85E | 66N | 3 | 4 | U | U | | |
| 26.4 | 1 | N78E | 65N | 2 | 9 | H | U | | |
| 27.4 | 1 | N68E | 70N | 5 | 4 | U | U | | |
| 27.9 | 1 | N82E | 70N | 3 | 10 | U | T | | |
| 28.6 | 1 | N75E | 62N | 1 | 7 | T | U | | |
| 29 | 1 | N72E | 72N | 1 | 4 | T | H | | |
| 29.3 | 1 | N88E | 70N | 1 | 9 | T | T | | |
| 33.2 | 1 | N88E | 80N | 3 | 11 | U | T | | |
| 34.8 | 1 | N85W | 74N | 2 | 3 | T | T | | |
| 36.7 | 1 | N88W | 84S | 7 | 3 | U | U | | |
| 38.6 | 1 | N56E | 75W | 1 | 8 | T | T | | |
| 39.6 | 1 | N60W | 54N | 5 | 1 | U | T | | |

### 6.2.11 SCANLINE 11

| | | | | | | | | | |
|---|---|---|---|---|---|---|---|---|---|
| Scanline Data | 070600 | | | | | | | | |
| Name | SCANLINE_11 | | | | | | | | |
| | | | | | | | | | |
| GPS points along the scan line | | | | | | | | | |
| Waypoint | Altitude | Scanline distance (ft) | | Leg | Orientation | | | | |
| 141 | 7013 | 0 | | | | | | | |
| 142 | 7013 | 33 | | 1 | 270 | 15 | | | |
| | | | | | | | | | |
| | | | | | | | | | |
| | | | | | | | | | |
| Rocktype | | | Red Peak Siltstone | | | | | | |
| | | | ft | in | | | | | |
| Stratigraphic thickness | | | | | | | | | |
| Bedding orientation | | | N50W | 42S | | | | | |

| | | | | | | | | | |
|---|---|---|---|---|---|---|---|---|---|
| DATA | | | | | | | | | |
| **Scanline length** | **Leg** | **Orientation** | | **Trace length** | | **Terminations** | | **Movement** | **Comments** |
| Ft (decimal) | | Strike | Dip | Ft | In | Upper | Lower | | |
| 1 | 1 | N71E | 42S | 1 | 10 | U | T | | most fractures |
| 1.9 | 1 | N38E | 76E | 0 | 9 | T | T | | have calcite |
| 3.1 | 1 | N11E | 86E | 0 | 12 | T | U | | filling in |
| 3.8 | 1 | N20E | 82E | 5 | 0 | U | U | | direction |
| 5.4 | 1 | N43E | 86E | 2 | 0 | T | A | | perpendicular |
| 6 | 1 | N30E | 74E | 0 | 6 | U | T | | to face |
| 6.8 | 1 | N29E | 76E | 5 | 3 | U | T | | |
| 6.8 | 1 | N47E | 50S | 4 | 5 | T | T | | |
| 8 | 1 | N20E | 57E | 0 | 5 | U | U | | |
| 9.5 | 1 | N12W | 52E | 0 | 9 | U | T | | |
| 10.65 | 1 | N15E | 76E | 1 | 11 | T | A | | |
| 9.9 | 1 | N90E | 25S | 5 | 8 | T | B | | |
| 11 | 1 | N25W | 68E | 2 | 3 | T | A | | |
| 12.2 | 1 | N18E | 68E | 4 | 5 | U | B | | |
| 12 | 1 | N58E | 72S | 1 | 8 | T | A | | |
| 12.9 | 1 | N39E | 70W | 1 | 10 | T | T | | |
| 13.5 | 1 | N46E | 59W | 0 | 10 | T | B | | |
| 13.9 | 1 | N27E | 90S | 5 | 4 | B | U | | |
| 14.1 | 1 | N50E | 55S | 2 | 5 | A | A | | |
| 14.9 | 1 | N20W | 50E | 0 | 6 | U | U | | |
| 15.1 | 1 | N14W | 60E | 0 | 8 | U | U | | |
| 16.1 | 1 | N30W | 62E | 2 | 2 | U | U | | |
| 17.5 | 1 | N20W | 52E | 2 | 8 | T | A | | |
| 19.9 | 1 | N09E | 55E | 1 | 7 | T | T | | |
| 20.1 | 1 | N21W | 78E | 2 | 8 | A | T | | |
| 20.9 | 1 | N05E | 82E | 2 | 3 | A | T | | |
| 21.6 | 1 | N55E | 48S | 1 | 9 | A | A | | |
| 23.5 | 1 | N17E | 83W | 2 | 0 | T | T | | |
| 21.7 | 1 | N51W | 52S | 3 | 2 | A | B | | |
| 23.8 | 1 | N39E | 76W | 1 | 4 | T | U | | |
| 24.5 | 1 | N11E | 61E | 4 | 3 | A | A | | |
| 25.7 | 1 | N20E | 68W | 1 | 9 | T | A | | |
| 26.7 | 1 | N28E | 70E | 1 | 5 | T | T | | |
| 27 | 1 | N52E | 67E | 6 | 0 | U | A | | |
| 28 | 1 | N59E | 30S | 5 | 8 | B | A | | |
| 29.3 | 1 | N25E | 71E | 1 | 6 | A | H | | |